


informatics inc 

FC


ADA 012790



DDC
RECEIVED
DEC 1 1975
D



ACCESSION FOR THE	
PTIC	WAVE BOOKS <input checked="" type="checkbox"/>
PTC	RAFF SULLIVAN <input type="checkbox"/>
WAVE SINGER	<input type="checkbox"/>
IDENTIFICATION	
BY	
DISTRIBUTION AVAILABILITY COVER	
DATE	AVAIL. and/or SPECIAL
A	

**EFFECTS OF
HIGH POWER LASERS,
NO. 6**

March - October 1975

Sponsored by
Defense Advanced
Research Projects Agency

DARPA Order No. 3097

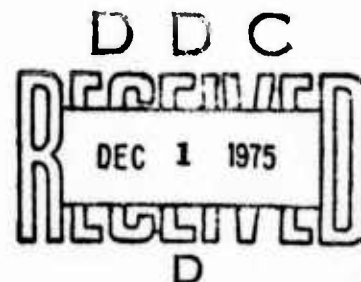
DARPA Order No. 3097
Program Code No. P6L10, P6D10, P6E20, P6G10
Name of Contractor:
Informatics Inc.
Effective Date of Contract:
September 1, 1975
Contract Expiration Date:
November 30, 1975
Amount of Contract: \$100,617

Contract No. MDA-903-76C-0099
Principal Investigator:
Stuart G. Hibben
Tel: (301) 770-3000
Program Manager:
Ruth Ness
Tel: (301) 770-3000
Short Title of Work:
"Laser Effects"

This research was supported by the Defense Advanced Research Projects Agency and was monitored by the Defense Supply Service - Washington, under Contract No. MDA-903-76C-0099. The views and conclusions contained in this document are those of the author and should not be interpreted as necessarily representing the official policies, either express or implied, of the Defense Advanced Research Projects Agency or the United States Government.

Informatics Inc

Information Systems Company
6000 Executive Boulevard
Rockville, Maryland 20852
(301) 770-3000



Approved for public release; distribution unlimited

REPORT DOCUMENTATION PAGE		READ INSTRUCTIONS BEFORE COMPLETING FORM
1. REPORT NUMBER	2. GOVT ACCESSION NO.	3. RECIPIENT'S CATALOG NUMBER
6 TITLE (and Subtitle) Effects of High Power Lasers, No. 6 March - October 1975		5. TYPE OF REPORT & PERIOD COVERED Scientific. . . Interim
		6. PERFORMING ORG. REPORT NUMBER
10 AUTHOR(s) St G./Hibben, J./Kourilo, M./Ness/ B./Shresta		8. CONTRACT OR GRANT NUMBER(s) MDA 2903-76C-0099
9. PERFORMING ORGANIZATION NAME AND ADDRESS Informatics Inc. 6000 Executive Boulevard Rockville, Maryland 20852		10. PROGRAM ELEMENT, PROJECT, TASK AREA & WORK UNIT NUMBERS DARPA Order 3097 Program Code No. P6L10, P6D10, P6E20, P6G10
11. CONTROLLING OFFICE NAME AND ADDRESS Defense Advance Research Projects Agency/TAO 1400 Wilson Boulevard Arlington, Virginia 22209		12. REPORT DATE November 12, 1975
		13. NUMBER OF PAGES 75
14. MONITORING AGENCY NAME & ADDRESS (If different from Controlling Office) Defense Supply Service - Washington Room 1D245, Pentagon Washington, D. C. 20310		15. SECURITY CLASS. (of this report) UNCLASSIFIED
		15a. DECLASSIFICATION/DOWNGRADING SCHEDULE
16. DISTRIBUTION STATEMENT (of this Report) Approved for public release; distribution unlimited.		
11 12 Nov 75 / 12 83p.		
17. DISTRIBUTION STATEMENT (of the abstract entered in Block 20, if different from Report)		
18. SUPPLEMENTARY NOTES Scientific . . . Interim		
19. KEY WORDS (Continue on reverse side if necessary and identify by block number) High power lasers Beam-target interaction Laser damage Optical breakdown Laser-plasma interaction		
20. ABSTRACT (Continue on reverse side if necessary and identify by block number) This is the sixth compilation of abstracts of Soviet studies on high power laser technology, covering material published from March through October 1975. Articles are grouped by laser interaction with metals, dielectrics, semiconductors, miscellaneous targets, and laser-plasma interaction.		

INTRODUCTION

This is the sixth compilation of abstracts of Soviet studies on high power laser technology, covering material published from March through October 1975. Articles are grouped by laser interaction with metals, dielectrics, semiconductors, miscellaneous targets, and laser-plasma interaction.

A first-author index and an index of source abbreviations are appended.

TABLE OF CONTENTS

Summary	iii
1. Metal Targets	1
2. Dielectric Targets	18
3. Semiconductor Targets	33
4. Miscellaneous Studies	43
5. Laser-Plasma Interaction.	51
6. List of Source Abbreviations	69
7. Author Index to Abstracts	75

SUMMARY

The laser interaction studies covered in this report are summarized briefly as follows.

Laser erosion of several metals in fluids, mainly water, was compared by Ageyev to effects in air, showing substantial differences in ejecta behavior. A study by Branov shows conditions for which a liquid rather than vapor phase can be the principal factor in crater formation. Bonch-Bruyevich claims novel results in laser "dielectrization" of a thin mercury film. Two papers by Buravlev test laser erosion as a function of ambient air pressure, heat treatment and plastic deformation of the target. Zhukov describes laser effects on wear and hardness properties of cast iron, and laser reduction of oxides is reported by Nepokoychitskiy.

Crater formation in group IV-VI transition metals and their carbides is discussed in two papers by Samsonov. Luk'yanov gives a theoretical treatment of laser vaporization of aluminum; factors controlling the geometry of laser-drilled holes are reviewed by Lobacheva. Papers by Larina and Smyslov report laser effects on crystalline and powdered molybdenum, including a comparison with shock wave effects. Pressure sensors for beam-target reaction are reported by Golubev, and Krylov gives specifications on a laser welder.

In dielectrics, Tribel'skiy develops a laser heating theory in terms of a temperature distribution function. Another theoretical treatment is given by Vincgradov on energy absorption by free electrons in a dielectric. A study of laser-induced dislocations and crack formation in dielectrics is presented by Larina; Kats analyzes the dielectric lens effect generated by a laser, and a model of laser effects on a thin-layer dielectric is discussed by Smirnov.

Breakdown from self-focusing in glass, quartz and other dielectrics is detailed by Ashmarin, using pulse holography. Buzhinskiy describes Nd glass laser breakdown of several commercial glasses; Aleksandrov reports similar threshold tests on PMMA as well as lead targets. Types of laser-induced stress in glass are analyzed in tests by Vigasin and by Andreyev. Threshold as a function of surface structure is discussed in one paper by Aleshin, and in another he shows the probabilistic nature of glass breakdown. Lokhov studies theoretical differences in damage to entrance and exit faces of high-power optical elements. Heating tests on high-quality optical glass are described by Bonch-Bruyevich, using an Nd glass laser.

In semiconductors, Bredikhin studies optical response in ZnS crystals stressed by intense light, and Brodin describes laser effects on photoelectric properties of CdS. Laser-induced diffraction in CdSe is reported in tests by Vaytkus. A theory on thermal breakdown in a semiconductor is suggested by Vitkin; Zolotukhin reports laser effects on an iron-silicon solution. Comparative damage to ZnS films from laser and electron beams is described by Amigud.

Miscellaneous beam-target studies include a laser induced metal-to-semiconductor transition observed by Kaminskiy, a theoretical model of e-m stress in solids by Gusev, and an analogous study by Apollonov to determine factors for increasing optical strength of laser elements. Karamzin gives a numerical study on mutual focusing of beams in nonlinear media. Tests are reported by Krylova on threshold characteristics of several oxide films, and by Malyarovskiy on ruby laser scattering by liquid CO₂. Laser techniques for forming grids, scales, etc. are described by Veyko. Pivovarov and Uglov summarize two conferences on high-energy optical interactions; Uglov also gives a theoretical study on heating of anisotropic materials.

In studies primarily concerned with laser plasma interactions, tests of a sustained optical discharge in xenon above a laser target are described by Arzuov. Bakeyev discusses spectra of laser flares from metal targets. Use of a laser beam for plasma diagnostics is evaluated in papers by Burakov and by Semenov. Electron spectra of a laser plasma are analyzed by Bykovskiy, and Karpov discusses electron and ion density in a plasma, based on scattering studies. Tests of laser breakdown in air are described by Dabu; other reports include one by Min'ko on laser plasma generators, and an analysis of trace elements in a laser flare, described by Zhdanov.

Theoretical studies on laser compression of thermonuclear targets are reported by Gol'din, Kaliski and Kryuchenkov; another paper by Gol'din treats characteristics of plasma dispersion from a CD target. Gamaliy discusses some techniques for producing spherical solid hydrogen and polystyrene targets for CTR studies, including use of rubber cement filaments to suspend the spheres. A combined spectroscopy and interferometry method is described by Zakharenkov which has been used to determine the very high electron densities in early stages of a laser plasma. Finally, Berezhnaya describes a polarimetry technique for laser plasma analysis, using a submillimeter laser.

1. Metal Targets

Ageyev, V. A. Study of optical erosion of metals in fluids. ZhPS, v. 23, no. 1, 1975, 42-46.

The author summarizes the results of laser cavity formation in a series of metals, comparing effects obtained in ambient air to those with the target in various fluids. A free-running Nd glass laser was used with energies up to 10j and pulse width of 140 μ sec. Tests were run with beam focused above, on and behind the target surface, at incident densities of 10^6 - 10^{10} w/cm².

Quantitative results are best seen in the table below, which lists all tested target metals and their crater dimensions, for varying focal settings and pulse energies, in both air and distilled water.

Other fluids tested included heptane, benzol, xylene, ether and glycerin, both the analysis is limited to the distilled water case.

Results show a general similarity in the character of crater formation, in terms of target parameters, whether the target is in air or liquid. In the initial or stationary phase comprising metal heatup and melting, there is no appreciable difference; in the second non-stationary phase with ejecta and vapor products exiting the crater, the liquid ambient understandably has a more pronounced effect. Boiling and shock wave propagation were observed in the latter case. Some metals, notably copper, were negligibly affected in the liquid ambient; thin foils of tantalum and molybdenum suffered only surface distortion in liquid.

The one qualitative comparison illustrated by the authors is shown in Fig. 1, comparing crater formation in lead for air and water ambients.

**Crater Diameter (d) and Depth (h) in Microns From Laser Exposure in
Air and Distilled Water**

Metal	Air						Water												
	on surface $\Delta F=0$			above surface $\Delta F=+1 \text{ MH}$			below surface $\Delta F=-1 \text{ MH}$			on surface $\Delta F=0$			below surface $\Delta F=-1 \text{ MH}$						
	Intensity, $E \cdot 10^4, \text{ W/cm}^2$						Focus:												
	1.75	11.8	1.75	11.8	1.75	11.8	1.75	11.8	1.75	11.8	1.75	11.8	1.75	11.8	1.75	11.8			
d	h	d	h	d	h	d	h	d	h	d	h	d	h	d	h				
Sn	160	240	350	310	90	120	170	180	390	420	580	180	97	400	106	180	103	450	121
Pb	170	500	420	810	100	280	190	470	200	600	990	190	150	480	186	230	262	480	230
Zn	150	100	330	150	70	—	130	60	170	160	200	170	33	390	56	190	52	400	50
Bi	180	1610	450	2340	100	410	160	630	210	1730	2510	210	187	540	198	240	295	560	313
Mg	100	—	210	80	60	—	90	—	130	—	240	120	23	260	34	160	36	300	40
Al	110	—	220	70	70	—	100	—	140	—	250	100	21	270	32	190	33	300	38
Cu	70	—	160	50	—	—	50	—	100	—	180	70	—	190	—	—	—	—	—
Mn	230	1760	510	2620	130	550	210	670	280	1980	2870	280	285	661	332	300	301	620	207
Mo	130	80	290	150	60	—	110	—	160	120	190	160	30	500	51	170	49	320	56
Ta	130	90	300	160	60	—	100	60	160	130	200	160	30	300	46	170	43	330	51
W	120	80	250	140	60	—	100	—	150	110	180	160	26	310	41	160	40	310	47
Wood's metal	160	410	570	660	120	140	150	230	190	350	530	190	105	430	142	250	112	470	138



Fig. 1. Sectional and top views of laser cavity in lead.

1, 2 - in air; 1', 2' - in distilled water.
 Energy = 6j, density = 11.8×10^8 w/cm²,
 $\Delta F = 0$.

Branov, M. S., B. A. Vershok, and I. N. Geynrikhs. Determining the depth of the fused region from the action of laser radiation on metal. TVT, no. 3, 1975, 566-572.

Baranov et al. question the excavation mechanism of laser cavity formation in metals as proposed by other authors. Specifically the present authors postulate that, within a certain range of incident power densities, the predominant mechanism is formation of a liquid phase at the crater bottom, rather than a vapor phase as suggested elsewhere. A theoretical model to this effect was developed, and experiments to test it were conducted.

Target metals were Sn, Zn, Ni and Ti, exposed to a quasi-cw focused beam from an SLS-10-1 source ($\lambda = 10.6 \mu ?$). Pulsed widths of 2 and 4 μs were used, at densities in the range of $0.7-14 \times 10^5 \text{ w/cm}^2$; incident energy was 0.7 to 10 j. A comparison of test results with theory for both vapor and liquid phase models is presented with power density plotted against rate of crater penetration. These confirm the liquid phase model for the cited range of test conditions. The authors include one example of crater formation in titanium for various beam intensities (Fig. 1).

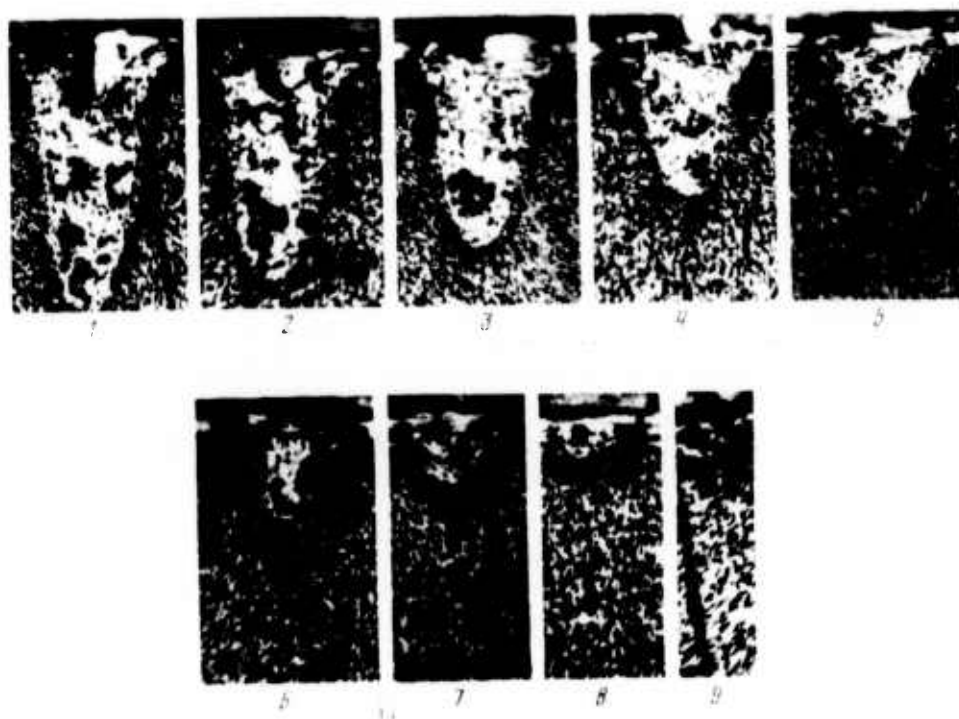


Fig. 1. Melt zone in Ti for various q ($\times 10^5 \text{ w/cm}^2$):
 1- 7.375; 2- 5.97; 3- 5.2; 4- 4.13; 5- 3.1; 6- 2.73;
 7- 2.215; 8- 1.1; 9- 0.59.

Bonch-Bruyevich, A. M., and S. Ye. Potapov.
Drop in metallic absorption of mercury under the
 action of intense optical radiation. ZhTF P, v. 1,
 no. 8, 1975, 353-359.

Experiments are described on "dielectrization" of a metal film

under a critical level of laser exposure. The work relates to an earlier proposed theory, suggesting that at some critical temperature a metal will transpose to a dielectric state. The authors used as a target a mercury film held between quartz plates, and exposed to square pulses from an Nd glass laser of varying pulse widths, and energy levels up to 300 j. The transition effect was observed by passage of light from a second source (a xenon arc lamp) through the mercury film.

Results are cited for film thicknesses of 30, 60 and 110 microns exposed to a focused laser spot of 6 mm diameter, and pulse widths of 0.1 - 2 μ s. At a critical range of energy density near damage threshold a pronounced transparency effect appears in the film, as registered by photomultipliers recording both reflected and transmitted light. Furthermore the bleaching effect lags the applied laser pulse, persisting for several hundred microseconds after the laser shot; the effect is repeatable. The critical energy range is not further identified other than being described as very narrow.

The authors claim this as the first direct experimental evidence of the bleaching of a metal under intense optical radiation, and urge further tests of the effect.

Buravlev, Yu. M., and B. P. Nadezhda. Effect of reduced atmospheric pressure on the erosion of metals under laser radiation. IN: Sb. Fizika tverdogo tela, no. 4, Khar'kovskiy Gos. un-t, 1974, 53-56.

Features of laser interaction with a metallic target were studied at various air pressures from room down to 10^{-5} torr. Target specimens used were Armco iron and type Shkh-15 steel. The radiation source was the Luch-1M laser, operating in a free-running regime with pulse energy of

about 2 joules and 2 millisecond duration. Targets were irradiated in a special chamber, in which the pressure was lowered incrementally with a fore pump and vacuum unit. Target erosion was determined by weighing the specimen before and after exposure, and was calculated in mg per pulse. Results are plotted in Fig. 1, where each point on the curve is based on an average of 60 pulses; errors in measurements were about 15%. External appearance, shape and longitudinal cross-section of the craters formed were also simultaneously studied.

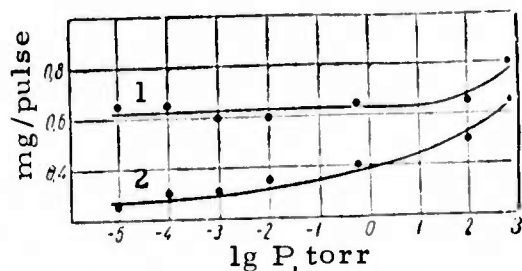


Fig. 1. Laser erosion of Armo iron (1) and Shkh-15 steel (2) as a function ambient pressure.

The results show interesting peculiarities in the relationship of laser erosion of metals with pressure. For example, for Shkh-15 steel, an increase of pressure from 10^{-5} torr to atmospheric leads to an approximate doubling of erosion, while this effect in the case of Armco iron is not very significant.

Buravlev, Yu. M., B. N. Nadezhda, and V. N. Seredenko. Effects of heat treatment and plastic deformation on laser erosion of metals and alloys. FiKhOM, no. 3, 1975, 30-35.

This is evidently an extension of the previous work, in which the authors continue to examine factors governing laser erosion of metals. Here a number of steel, iron, aluminum, titanium and copper alloys were

tested under various preheat or prestress conditions. The test apparatus was the same as in the foregoing paper.

A general result of these tests was that erosion in previously annealed or cold-worked specimens was 25-30% greater, for a given beam exposure, than for untreated specimens. The three-sigma criterion was used for significant erosion difference, with rms measurement error estimated at 15 to 20%. The reason advanced for the observed difference is ascribed to increased internal stress and/or lowered thermal conductivity of the treated specimens, both of which factors would enhance crater formation. Fig. 1 shows craters formed in a titanium alloy.



Fig. 1. Microstructure of crater region after exposure of VTS titanium alloy.

a- annealed, b- prestressed specimen; x530.

The tests also show that laser action on alloyed targets will have a selective effect depending on the physicochemical structure of the target material.

Zhukov, A. A., A. N. Kokora, D. D. Timonich,
 V. K. Tomas, B. N. Kolesnikov, O. P. Orlov,
 and N. S. Goryachev. Surface hardening of cast
 iron parts by laser radiation. F-KhMM, no. 1,
 1975, 84-85.

Laser hardening of cast iron surfaces was experimentally investigated by using cast iron specimens containing 3.4 - 3.6% C, 2.2 - 2.6% Si, 0.4 - 0.5% Mn, 0.10 - 0.25% P, and up to 0.14% S by weight. Laser irradiation of bearing surfaces was done with the GOS-100 M (pulse energy 50-200 joule) and UL-20 devices (pulse energy 10-20 joule). Pulse duration did not exceed 6 μ sec. Power density in the exposed regions was varied over the range $10^4 - 10^5$ watt/cm² by using different stages of radiation focusing. Irradiation spots were located on the specimen surface successively one after another with little overlapping.

Tests were conducted for hardness and durability of the specimen before and after laser exposure. Hardness of the initial cast iron was $HV_5 = 262$, while after laser hardening it was measured at 666 - 677. Durability of specimens was tested under different applied pressures, with the results shown in the table below. It is seen that wear of the laser

State of specimen	Wear, mg/cm ² . m (for 1000 m track) under pressure				
	pressure: 15 kg/cm ²	30	50	75	100
Before laser irradiation	250	288	300	315	338
After laser irradiation	52	170	220	288	330

irradiated specimen approaches that of the nonirradiated with increase in pressure.

Nepokoychitskiy, A. G., and P. A. Skiba.

Some principles in reduction of metal oxides by laser radiation. ZhPS, v. 22, no. 1, 1975, 37-41.

An experimental study is made of metallization of a metal oxide surface in a protective reducing medium (glycerin), using type GSI-1, LDTI-68, and K-3M ruby and Nd glass lasers, as well as a 100 w CO₂ laser. Powdered Ni, Cu, Co, and Fe oxides and M400 HH ferrite specimens compacted and sintered in the form of 1 mm thick plates, were subjected to laser radiation at power densities below breakdown threshold. The form and structure of the metallic coating thus produced on the plate surface, or on hole surfaces, varied with change in laser generation mode, beam focusing, pump energy, and specimen porosity.

A continuous, uniform metal coating was obtained on a plate surface exposed to the c-w CO₂ laser. Width and thickness of the metallic band produced on a rotating specimen surface by a focused beam from a free-running LDTI-68 Nd glass laser varied with rotational speed. Empirical formulas are given describing variations of metal coatings on the walls of blind and through holes produced by different focusing of the K-3M laser [unidentified] beam. Regularities were noted in variations of the hole parameters and depth of the wall coating produced by a laser beam focused on the oxide plate surface. Several photos of hole formation are included.

It is concluded that the geometry and properties of metal coatings can be controlled by varying experimental conditions, mainly laser generation mode, and speed of beam or specimen motion. The described technique is applicable to oxide welding and bonding.

Samsonov, G. V., A. D. Verkhoturov, V. S.
Kovalenko, V. P. Kotlyarov, and A. I. Roshchina.
Laws of the destruction of metals during laser
processing. EOM, no. 6, 1974, 14-16.

This work investigates the effects of material characteristics on the nature of transition metal destruction under laser exposure. Transition metals of groups IV-VI were treated in the SLS-10-1 laser device at a radiation wavelength of $10,600 \text{ \AA}$, pulse duration 1.5 millisecc, radiated power of 1 kw and flux density, $1.3 \times 10^6 \text{ watt/cm}^2$. After irradiation in a single-pulse regime, specimens were cut on an electric arc machine to obtain diametrical cross-sections of the resulting holes.

Relationships of the hole volumes were determined and plotted as a function of: 1) heat of fusion; 2) heat of sublimation; 3) melting point; and 4) number of electrons in the d-shell. It was noted that the increase of electrons in the d-shell up to 5 reduces the volume of ejected materials in the tested metals. However, increase over 5 leads to a lowering of erosion resistance of the metals, which is associated with the increase of statistical weight of atoms with less stable d^{10} configuration; their workability is also improved. This tendency was observed in metals irrespective of the laser treatment regime.

In conclusion, it is pointed out that the volume of ejecta decreases with increase of valence electron localization in stable configurations; with the increase of energetic stability of these localizations; and with lowering of the probability of their destruction because of valence electron transitions at deeper levels.

Samsonov, G. V., A. D. Verkhoturov, V. S. Kovalenko, N. I. Prikhod'ko, and V. Ya. Naumenko. Factors governing erosion of carbides of group IV-VI transition metals by laser beam. EOM, no. 2, 1975, 11-13.

In an extension of the foregoing work, the authors report test results on laser erosion of numerous carbides of IV-VI group metals. The laser used was a standard SLS-10-1 type, with specifications of 1.3×10^6 w/cm² density, 1.5 millisecc pulse width, $\lambda = 10.6 \mu$ and $f = 37$ mm. Tests were run on pressed sintered specimens which were cured at 1400-2340C for several hours. The weight loss of a specimen by erosion was the criterion for comparison, and showed that the greatest loss occurred in group IV carbides (TiC, ZrC), and least in the VI group, as shown in the table.

Laser Erosion of Carbides

Carbide	TiC	ZrC	HfC	VC	NbC	TaC	Cr ₃ C ₂	Mo ₂ C	WC
Erosion $\Delta er \times$ $\times 10^{-6}$, g x mol	102,0	65,0	9,0	55,0	10,8	9,0	3,0	4,5	2,3

The results further show that erosive quality is not a function only of thermal properties, but also of mechanical factors such as lattice rigidity, modulus of elasticity, and microhardness. In these tests, microhardness showed the clearest correlation with erosion level. For a better interpretation of erosive effects the authors examine electron states of the carbides, specifically the effect of localized valence electrons. The comparative effect of the latter on laser erosion is seen in Fig. 1. Test evidence suggests that erosion resistance is determined mainly by brittleness in group IV, but by chemical bonds in group V and VI carbides.

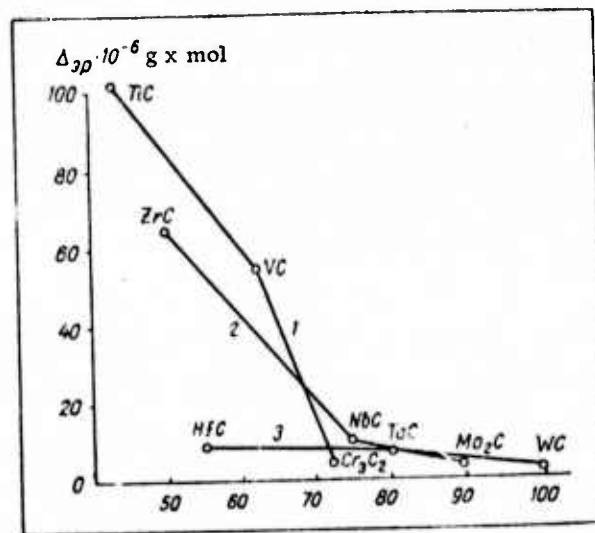


Fig. 1. Erosion of carbides vs. degree of localization of valence electrons.

1- group IV; 2- group V; 3- group VI.

Luk'yanov, A. T., and P. G. Itskova.
Numerical solution to the problem of pulsed vaporization in vacuum. TVT, no. 1, 1975, 235-237.

Interaction of moderately intense (10^5 to 10^6 w/cm²) laser radiation fluxes with an aluminum surface is analyzed. The problem of pulsed vaporization of metal in vacuum is formulated as difference equations analogous to partial differential heat equations. The difference equations are solved by integration, using statistical simulation by two-dimensional electric circuits.

The initial data are presented and the solution is obtained in graphical form by shifting the input device of decision element along a curve. The plots thus obtained show two consecutive stages of pulsed vaporization in vacuum. In the first stage, heat of vaporization $Q_v(T_s)$ is much smaller

than heat input to the surface so that all absorbed energy is used for heating; temperature gradient is the highest at the surface and vaporization is negligible. In the second stage, $Q_v(T_s)$ increases with increase in surface temperature T_s ; this increase is limited by the amount of absorbed energy. The maximum temperature gradient then shifts inward into the metal; the quantity of vaporized material can be calculated. In the given example the authors show that to obtain vaporization of an aluminum surface absorbing at a 10^5 w/cm^2 rate the pulse width should be 10^{-3} sec.

Lobacheva, G. Ya., and B. S. Slavin.
Determination of processing regimes for
obtaining profile apertures in opaque materials
by focused laser radiation. FiKhOM, no. 1,
1975, 6-9.

The extremal deviations of a laser hole profile from the dimensions and shape of the focused laser spot are evaluated, with a allowance for thermal characteristics of the material (steel or ceramics) and the laser beam parameters. The evaluation is based on an ideal model of melt accumulation on the hole walls during laser pulse duration τ . The laser boring process is considered as the result of two competing processes: wall material melting and melt ejection from the exposed zone.

The maximum (y_{\max}) and minimum (y_{\min}) width of the hole and melt volume at a given time are formulated. It is shown that the minimum deviation of cross-sectional dimension $\Delta = r - y_{\min}$ can decrease to zero with drop in radiation intensity, i. e., the hole may be closed by melt. The conditions preventing hole closing are formulated. Dispersion of hole dimensions is represented by the area bounded by the $y_{\max}(\tau)$ and $y_{\min}(\tau)$ curves. The cited formulas and plots indicate that Δ_{\max} depends on thermal characteristics of the material, and that τ and Δ_{\min} depend also on the

specimen thickness and radiation intensity. It is concluded that precision boring in metals is feasible only by using short pulses and high intensity radiation.

Larina, R. R., and L. I. Mirkin. Dislocations in molybdenum after laser irradiation. IVUZ Fiz, no. 4, 1975, 159-160.

Results are summarized of a study of dislocation structures in molybdenum single crystals after their laser irradiation. Density of deformed dislocations in the laser interaction region was calculated with the help of a scanning electron microscope.

It is shown that destruction of old and formation of new boundary regions takes place along with increase in deformed dislocation density near the laser crater.

The resulting dislocation structure is associated with the 'thermal' mechanism of plastic deformation and destruction during laser radiation.

Smyslov, Ye. F., G. V. Davydov, and Ye. P. Alebastrova. X-ray diffraction and micrographic studies of molybdenum after exposure to shock waves and a laser beam. DAN B, no. 5, 1975, 435-438.

Structural transformations caused in powdered Mo specimens by the effects of shock waves and laser pulses were studied to gain information on shock wave and laser beam interaction with solids, particularly with

respect to high temperature effects. Shock compression to 500-700 kbar was produced by a glancing detonation wave from ammonite charge detonation. A GOS-30 M laser emitting 10^{-3} sec. pulses at up to 30 j was also used. The powdered specimens were sintered into compact solids either by shock compression or by laser beam irradiation. Fine structure of the compacted specimens was determined from macro- and micrographs and X-ray powder diffraction patterns.

The similarity between microstructures of the central regions of shock-compressed specimens and those of the laser-treated zone led to the conclusion that high-speed melting and solidification are involved in both cases. Analysis of the X-ray diffraction pattern revealed significant differences in fine structure between the central and peripheral regions of the shock-compressed specimens and between the latter and the laser-exposed specimens. The difference in broadening of powder diffraction lines between two regions of shock compressed specimens is attributed, in agreement with microhardness data, to a preponderance of broken-down coherent scattering regions in the central zone, and microdeformations in the peripheral zone. The line broadening profile is approximated by an intensity distribution function of scattering angles. Photos are included showing both macrostructural and microstructural defects.

Golubev, G. P., I. Sh. Zlatin, T. N. Malashenko, and V. P. Filippov. Measuring pressure from the effect of a giant laser pulse on metal targets. IN: Sb. Metrologiya i metody optikofiz izmereniy. Moskva, 1974, 7. (RZhF, 1/25, no. 1D1184). (Translation)

A pressure gauge is described for pressure developed from the effect of a 100 to 150 nsec giant laser pulse at 10^7 w maximum power. The peak pressure was several hundred atmospheres.

Golubov, G. P., T. N. Malashenko, A. M. Pavlov, and V. B. Filippov. Pressure sensor for measuring the action of laser radiation on matter. IN: Sb. metrologiya i metody optikofiz. izmereniy. Moskva, 1974, 4-5. (RZhF, 1/75, no. 1D1183). (Translation)

A pressure sensor with a response time of 10^{-6} sec is introduced for recording rapidly changing pressures and pulse recoil from the interaction of laser radiation at $10^7 - 10^8$ w/cm², duration of 10^{-3} to 10^{-5} sec, with matter. The range of pressures generated by the laser plasma is 1 to 100 atmospheres.

Krylov, K. I., A. S. Mitrofanov, L. N. Stepanov, and A. S. Tsarev. A laser technological device. IVUZ Priboro, no. 2, 1975, 108-110.

Specifications are given for the LTU-1 laser system, which was developed and constructed by LITMO (Leningrad Institute for Precision Mechanics and Optics) for precision welding, heat treatment of thin films, and related tasks. Fig. 1 gives a functional diagram. Specifications are:

Pulse energy	-	not less than 2 joules.
Pulse duration	-	not less than 8 nsec.
Pulse repetition frequency	-	10 pulse/min.
Active element	-	neodymium glass, diameter = 6 mm and length = 100 mm.
Consumable power in a pulse	-	not more than 40 kva.
Cooling of active element	-	water or air.
weight	-	350 kg.

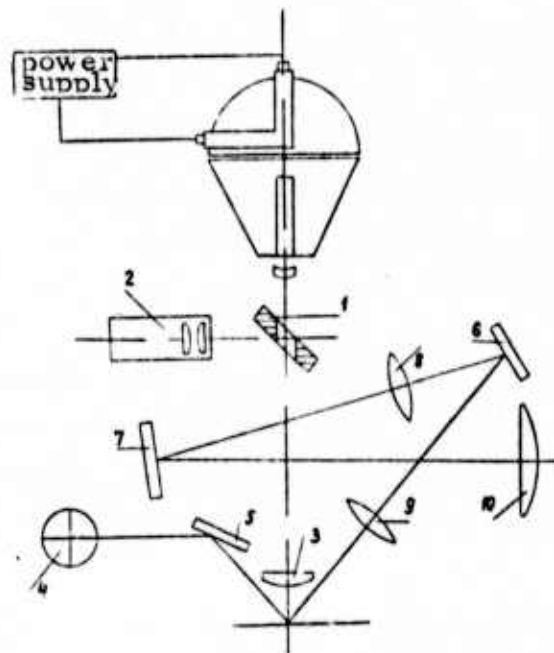


Fig. 1. Optical Schematic of the LTU-1 Laser.

1, 5, 6, 7- mirrors; 2- illuminator; 3- focusing lens;
4- condenser (microscope); 8- eyepiece; 9- objective;
10- screen.

The considered laser device is intended for:

- 1) welding of intracircuit joints in microelectronics,
- 2) precision instrument manufacturing technology,
- 3) computer technology,
- 4) local heat-treatment of thin films, and
- 5) correcting film magnetic matrices.

2. Dielectric Targets

Tribel'skiy, M. I., and A. Yu. Grosberg. Laser heating of a transparent medium with radiation-absorbing random inclusions. ZhETF, v. 68, no. 3, 1975, 1060-1065.

The frequency distribution function $P_{x,t}(T)$ of temperature is calculated for a transparent medium, such as a dielectric, with randomly distributed inclusions of arbitrary size which absorb laser radiation. The normalized frequency function $P_{x,t}(\theta)$ is expressed in integral form.

Calculation of the integral shows that under realistic conditions the unknown θ (hence T) distribution differs from Gaussian and is determined mainly by large-size inclusions. The boundary value problem is solved for three particular cases: $T - \bar{T} \rightarrow -\infty$, $T - \bar{T} \rightarrow 0$, and $T - \bar{T} \rightarrow \infty$, where \bar{T} is the mean temperature. In the latter case, the shape of $P_{x,t}(T)$ versus T curve is determined by the variation pattern of the frequency distribution function $f(R)$ only when the inclusion dimension $R \rightarrow \infty$, and is independent of heat-exchange conditions at the boundary. Application of the calculated distribution function is illustrated by evaluation of the mean volume $v(t)$ of a substance melted in time t .

Vinogradov, A. V. High-intensity light absorption by free carriers in dielectrics. ZhETF, v. 68, no. 3, 1975, 1091-1098.

Formulas are derived for the average rate $d(\epsilon)/dt$ of energy increase of a free (conduction) electron in a transparent dielectric in a high frequency electric field. The energy of a strong electric field generated

by high-power laser pulses and absorbed by an electron induces electric breakdown in a dielectric by the mechanism of avalanche ionization. This mechanism is described by the classical Boltzmann equation, with no restriction on the field strength E . Free electron interactions with longitudinal acoustic and polar optical phonons are taken into account in evaluation of $d\epsilon/dt$.

The final formulas of $d\epsilon/dt$ for an electron with given energy are derived in two particular cases of circular ($E_1=E_2=E, E_1 \perp E_2$) and linear ($E_2=0, E_1=E$) polarizations. The formulas show that a strong field affects frequency of the electron-phonon collisions. Consequently, an additional term in the $d\epsilon/dt$ formulas expresses $d\epsilon/dt$ dependence on E . Validity criteria of the classical approximation are formulated. The analytical formulas derived from the classical theory were found to be in agreement with quantum mechanical calculations of the absorption coefficient as a function of E (Pazderskiy, FTP, no. 4, 1972, 758).

Larina, R. R., and L. I. Mirkin. Thermal mechanism of plastic deformation and fracture of crystallized dielectrics from the effect of a laser beam. NM, no. 3, 1975, 447-449.

Electron microscope techniques are described for study of laser-induced reactions in dielectrics. Density (n) of laser-induced dislocations in sodium chloride single crystals was measured on electron micrographs of dislocation etch pits in the region of a 6 to 7 mm radius from the crater center. A GOS-30M pulsed laser beam was focused on the (100) cleavage surface. Pulse energy was 30 j maximum and pulse duration, 1 millisecond. Several concentric zones of different n and with different crack orientation were observed within the cited radius. Density n decreased nonuniformly from $\sim 10^9$ to 10^4 cm^{-2} with increase in radius. Measurement of n as high as 10^9 was obtained by increased magnification to 10,000 and using an appropriate etching technique.

Cracks due to the thermal effect of laser radiation were detected in the region of solidified melt by scanning the irradiated surface with the electron microscope at different magnifications. The cited observations made it possible to clarify the thermal mechanism of deformation and fracture of ionic crystals from laser beam effects. Delayed fracture, i. e., crack formation after laser cutoff, is seen as a peculiar property of brittle dielectrics.

Kats, A. V., and V. M. Kontorovich. Lens effect due to optical pressure on the surface of a transparent dielectric. ZhETF, v. 68, no. 2, 1975, 698-710.

Formation of a lens by bending of a liquid dielectric surface, and dynamics of the surface under pressure p_1 of a laser pulse, are analyzed in connection with the recent experimental detection of surface self-focusing of a laser beam and the concurrent lens effect due to p_1 . Lens shape is defined by a surface deflection $\zeta(r, t)$ where r is lens dimension and t is pulse length. In the most general case, $\zeta(r, t)$ can be determined from linearized hydrodynamic equations and p_1 is defined as the jump of the Maxwellian strain tensor. A single expression of $\zeta(r, t)$ describes both the lens shape and its dynamics. Space- and time-dependence of lens motion are examined separately. An extensive treatment is given expressing lens formation as functions of laser energy and pulse duration.

Ashmarin, I. I., Yu. A. Bykovskiy, V. A. Gridin, V. F. Yelesin, Ya. Yu. Zysin, A. I. Larkin, and V. A. Furmanov. Role of self-focusing in the destruction of transparent dielectrics by laser radiation. ZhETF, v. 68, no. 2, 1975, 562-567.

Initiation and dynamics of breakdown development in transparent dielectrics irradiated by giant ruby laser pulses is studied by pulse holography.

The experimental method is described and some new results are presented and discussed. A Q-switched laser emitting 2j pulses of 15 nsec duration was used in single or multimode operation. The laser pulse was focused into the bulk of the target specimen by lenses with 18, 36 and 85 mm focal distances.

It is shown that in a broad range of dielectrics (K-8 glass, fused quartz, lithium niobate, water) breakdown is initiated by a nontransparent filament formation in the focal region, irrespective of the focusing lens used and other experimental conditions. Time resolution in determining initiation of filament was about 1 nsec. The origin of filaments may be connected with radiation self-focusing which occurs when breakdown threshold is attained. The resulting filamentary structure exhibits a series of discrete eruptions which propagate over the entire focal region. These eruptions create shock waves which cause breakdown outside the focal region. It was established that breakdown threshold in glass and quartz is determined by energy accumulation (inertial process) whereas in lithium niobate it is determined by radiation power (inertialess process). The authors include a sequence of photos illustrating the breakdown process in K-8 glass.

Smirnov, V. N. Effect of optical radiation on a plane-parallel layer of an elastic medium. ZhTF, no. 2, 1975, 405-410.

The effects of stationary and pulsed radiation on a plane-parallel layer of transparent material, e. g., optical components, is examined, on the assumption of a Gaussian distribution of power density across an optical beam. Temperature T and the components σ_r , σ_z , σ_φ and τ_{rz} of the elastic stress tensor σ in the layer are formulated, using the system of cylindrical coordinates r , z , and φ and a Hankel integral transform to solve the equations of the T field.

Approximate expressions of T and σ components are derived for the particular case of a beam radius significantly greater than the layer thickness, $l/q > h$. In this case, a planar-stressed state is realized. The computed and graphically illustrated T and σ component distributions at different q values show that in the case of $l/q < h$ the stress state is not planar, and hence the planar-problem methods of the theory of elasticity cannot be used.

Buzhinskiy, I. M., A. Ye. Pozdnyakov, and S. A. Ushakov. Nature of optical surface destructions of some glasses at large interaction cross-section by short light pulses. OMP, no. 2, 1975, 46-49.

Experiments are described on destruction of optical glass surfaces by short laser pulses. A neodymium laser was used with an energy = 70 - 80 joules and pulse duration $\tau = 40$ nsec. Radiation was focused on target by a plane-convex tapered lens with focal length $f = 215$ cm. The diameter of the focal spot and its cross-section were $d = 1.55$ and $s = 1.88$ cm² respectively. Specimens used were K8, GLS and F8 glasses with standard grinding and polishing in resin. Threshold destruction was determined and character of optical surface destruction was studied.

The character of the observed optical destruction of glass surfaces is shown in Fig. 1.

The threshold destruction of a polished K8 glass exit surface for single exposure was $Q_{av} = 21.5$ joules/cm². When the threshold Q_{av} was increased by 30-40%, point cratering were seen to develop, with diameter = 0.1 - 0.2 mm and located irregularly over the surface at 1-2 mm intervals. At 30 joule/cm², characteristic circular spots with diameters around 0.5 mm

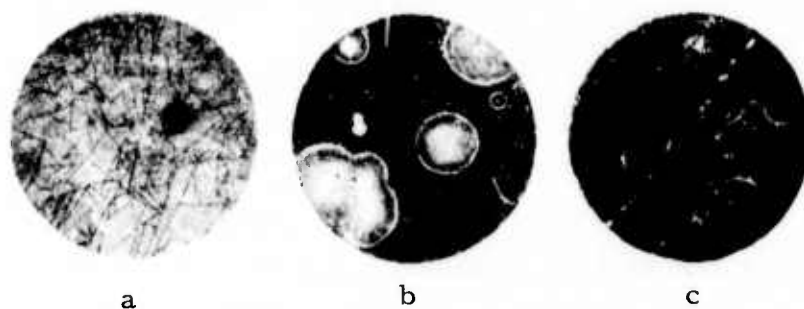


Fig. 1. Character of optical surface destruction of glasses at $\tau = 40$ nsec and $S = 1.88 \text{ cm}^2$.

(a) Front surface of K8 glass; (b) Back surface of GLS glass; (c) Back surface of F8 glass. Magnification 30x.

were formed on the front surface; an increase up to $50\text{-}60 \text{ joule/cm}^2$ led to formation of dense surface fusion. The destruction character of GLS and other neodymium glasses (silicate and phosphate) was similar to K8 glass. Threshold destruction of GLS equalled 15.9 joule/cm^2 . In the case of F8 glass the threshold was 11.2 joule/cm^2 . Increase of intensity by 20-30% caused formation of chips of 0.1-0.3 mm; sometimes chains of chips were observed extending along a single line (Fig. 1c).

Detailed discussions are given of the observed experimental results and general conclusions are drawn. It is noted that the determining factor for destruction of optical glass surfaces by short light pulses is the chemical stability of the glass together with its surface treatment.

Aleksandrov, V. I., and A. G. Solov'yev. Effect of spatial distribution of laser radiation on the destruction of condensed media. FiKhOM, no. 1, 1975, 3-5.

The space-time distribution of laser radiation and its interaction with substances were previously studied by the authors (FiKhOM, no. 4, 1973, 30-31). The present work conducts further investigations on the same topic and studies the effects of controlled spatial nonuniformity of

pulsed radiation with wavelength = 1.06μ on the destruction characteristics of polymethylmethacrylate (PMMA) and lead.

Experiments were conducted with neodymium laser, operating in a periodic or c-w regime. Radiation energy was 100-200 joules at a pulse width of 1μ sec. Descriptions are outlined of the experimental procedure. Relationships are found for the threshold destruction value of energy density as a function of the conditions of radiation focusing on PMMA. Dimensions are estimated of the nuclei which lead to crack formation. Conditions of radiation focusing on lead are also determined for which the specific recoil momentum of vapors and the destructive work function do not depend on spatial distribution.

Vigasin, A. A., S. A. Kazakev, I. V. Krasnov,
D. P. Krindach, B. A. Reznikov, and A. P.
Sukhorukov. Elastic, viscoelastic and residual
stresses in solids, resulting from c-w laser
radiation. ZhTF, no. 2, 1975, 411-419.

This article reports experimental and theoretical investigations of thermoelastic, viscoelastic and residual stresses arising in a glass plate as a result of c-w laser irradiation. The target used was a thin plane-parallel glass plate of dimensions $40 \times 40 \times 1.3$ mm; the plate was irradiated by a CO_2 laser with beam radius = 1.5 mm at a constant radiation power of 10 w, and exposure times up to a few seconds. Radial relationships were determined for the induced birefringence which was measured during as well as after exposure and cooling of the specimen. Birefringence in the first case is associated with temperatures stresses and in the second-residual.

Interpretation of the obtained results enabled the authors to plot the complete dynamics of stress formation up to the point of glass destruction, and values of these stresses were determined. Under weak laser exposure, when the glass softening point is not yet reached, stresses were of elastic character. At temperatures higher than the softening point ($T > 500$ C),

stresses were viscoelastic. It was found that stress values could attain enormous magnitudes (up to 2000 kg/cm^2), which leads to surface deformation, birefringence, changes in refraction coefficients in the radial direction due to piezo effects, and in the extreme case, destruction of the glass plate itself. The problem of stress formation in the glass specimen is also theoretically discussed using a viscoelastic model of a Maxwell medium with a sharp boundary of the softening zone. Calculated results are in good agreement with experiments.

Aleshin, I. V., G. D. Dvornikov, Ya. A. Imas,
V. I. Proshin, V. S. Salyadinov, and A. V.
Shatilov. Relation of the threshold optical break-
down of glass with its structure OMP, no. 3,
1975, 17-20.

The present work investigates the relationship of the threshold optical surface and internal breakdown of glasses as a function of a structural factor R . Here $R = N_o / N_{si}$, where N_o - nos. of oxygen atoms and N_{si} - nos. of glass-forming (silicon) atoms during irradiation by smooth laser pulses of nanosecond to millisecond durations. It was found that there is a general tendency toward lowering of the breakdown threshold of glass (surface as well as internal) with increase in the R -factor.

In case of internal breakdown this relationship is very obvious, while for surface breakdown there is a lesser tendency of lowering the threshold with increase in R . The observed character of relationships between the breakdown threshold and the glass structure is evidently due to changes of structurally-sensitive properties in glass, e. g. the softening point, light absorption at $\lambda = 1.06\mu$ and in the UV region, refractive index, and elastic modulus.

Andreyev, V. G. Directional crack-formation in glasses under the action of CO₂ laser beam.

I-FZh, no. 4, 1975, 739.

Experimental studies on the interaction of a focused CO₂ laser beam on a rotating glass tube showed that over a certain time a uniform circular crack occurs, which splits the tube into two parts. This effect is theoretically studied by considering the interaction mechanism of a laser beam with a glass tube up to phase transition, the glass tube being at a uniform initial temperature with no internal cooling. Expressions are derived for temperature, and its distribution over the middle plane in inner and outer surfaces of the tube is plotted as a function of time. It is seen from these curves that at time $t \approx 1$ sec, a quasistationary distribution occurs of temperature vs. thickness.

Heating of the tube gives rise to thermoelastic and bending stresses on it; expressions are derived for these stresses, taking into account temperature fields. Results indicate that thermoelastic stresses were significantly greater than bending stresses. Distribution of thermal stresses along radial coordinates is plotted, and comparisons are made with limits of the material strength. It is shown that destruction of the glass tube in the form of circular cracks occurs at the inner surface under the action of tangential tensile stresses, and propagates towards the external walls owing to axial tensile stresses.

Lokhov, Yu. N., V. S. Mospanov, and Yu. D. Fivevskiy. Evaporation and destruction of the end faces of solid transparent dielectrics by laser single-pulses. KE, no. 5, 1975, 898-901.

A series of previous experiments has shown that a significant difference exists in the nature of destruction of the entrance and exit faces of solid transparent dielectrics, when high-intensity laser pulses pass through

them. It has been observed that the incident surface fuses strongly and destruction takes place in the form of a plane cavity surrounded by cracks, whereas splitting of the surface and chipping tend to occur on the exit face.

The present work considers the evaporation process of the entrance face as well as the chipping off of the outlet face of a solid transparent dielectric under the action of a single laser pulse. An attempt is made to explain the effect of the direction of incident laser pulse on the character of its energy absorption by the dielectric surface. The authors conclude that the character of the destruction process is largely determined by absorption of laser radiation in the surface layer region as a result of avalanche electron multiplication. The main mechanism of the entrance face destruction is the evaporation of its surface; evaporation rate and threshold are calculated. It is shown that asymmetry in destruction of the entrance and exit faces is caused due to the attenuation of radiation during its passage through the absorbing heated surface layer; this leads to the displacement of the radiation absorption peak in the surface layer region. Heating of the substance at absorption peak causes an explosion under the surface, and this leads to chipping of the outlet face and ejection of heated materials. Sample calculations are given for a sapphire specimen, which was irradiated by ruby laser single pulses; theoretical results are in good agreement with experiments.

Bonch-Bruyevich, A. M., Ya. A. Imas, V. L. Komolov, V. S. Salyadinov, and V. N. Smirnov.
Character of absorption and heating of an optical glass by quasicontinuous Nd laser pulses. ZhTF, no. 5, 1975, 1117-1121.

Heating of type K-8 optical glass by quasicontinuous Nd laser pulses was investigated in a wide range of total pulse energy variations at a fixed pulse shape. The experimental method was described in a previous work of Bonch-Bruyevich et al. (ZhTF, v. 44, 1974, 463), and a brief description is outlined of the procedure in the present work. Quasicontinuous Nd laser radiation pulses with duration ~ 2 msec were focused on the target

with a lens $f = 250$ mm. The form of intensity distribution over the focal plane was close to Gaussian, and remained effectively unchanged throughout the pulse duration. Laser radiation energy was varied from 50 to 600 joules. Refractive index δ_n was determined by means of a Michelson interferometer, and the change of temperature at the axis of the focal region, ΔT_0 , was calculated at pulse termination for different pulse energies.

Within the considered energy range, experimental relationship $\Delta T_0(W)$ was found to be linear (Fig. 1). It was found that the absorption

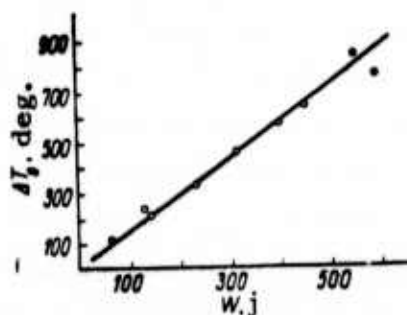


Fig. 1. Change in temperature of the glass, ΔT_0 , at the center of focal region at time t_0 as a function of total pulse energy.

coefficient α of the glass is independent of W and remains constant up to the point when irreversible structural damage is observed in the glass volume.

The authors point out that the method used to determine temperature in the present work can be used to measure small absorption coefficients (10^{-2} - 10^{-5} cm^{-1}), since it does not require high quality specimens of large dimensions. In addition, this method enables data to be obtained on local changes of absorption coefficient, which is highly desirable for the study of absorbing microdefects. This is also applicable for investigating large changes of absorption coefficient during laser radiation interaction, because in this case errors which result from radiation scattering due to refractive index gradient, and which are unavoidable in the method of measuring absorption coefficient by transmission, are totally absent.

Aleshin, I. V., A. M. Bonch-Bruyevich,
Ya. A. Imas, and V. L. Komolov. Probability
of optical breakdown of a glass surface. ZhTF,
no. 6, 1975, 1264-1267.

The proposition that optical breakdown in a transparent dielectric has a probabilistic rather than strictly threshold nature is tested. To do this the incident laser radiation was directed through a matrix to the target surface, so that a large number of focal spots of 100 micron diameter was simultaneously applied. The pattern of breakdown spots could then be evaluated with different laser intensities and target specimens. The authors used a low threshold glass, type F-2, so as to minimize optical stress on the matrix optics. A pulsed laser with 150 nsec duration was used.

Fig. 1 shows examples of breakdown patterns for different

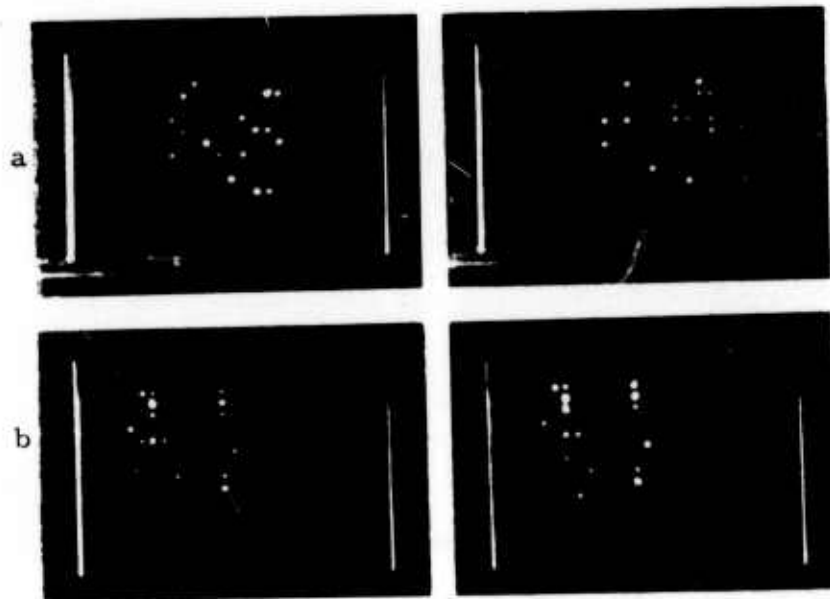


Fig. 1. Integral photos of laser breakdown
in F2 glass.

a- different target areas exposed; b- repeated
exposure of one area.

test conditions. With fresh areas of glass exposed the integral pattern changed, but the average number of breakdowns varied with laser power. Repeated exposure of the same area at fixed intensity levels showed that the integral breakdown pattern tended to repeat from one test to the next. A comparison of test results with theoretical breakdown probability as a function of laser intensity (Fig. 2) shows reasonable agreement in view of

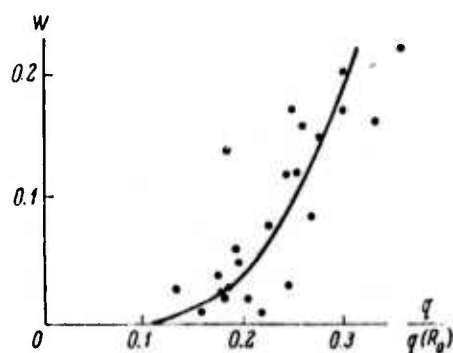


Fig. 2. Breakdown probability vs. laser power. Solid curve is from theoretical model.

the small number of test samples. The experiment hence is seen as verifying the proposed statistical model for breakdown.

The authors do not go further into dielectric breakdown mechanics, other than to define three main types of nonuniformity causing breakdown: 1) large scale variation in chemical composition; 2) micro-inclusions of metal or ceramic entrained during manufacture; 3) discontinuities caused by mechanical effects on the material. Some of these effects are not readily observable, and must be deduced from the breakdown process.

Darvoyd, T. I, Ye. K. Karlova, N. V. Karlov,
 G. P. Kuz'min, I. S. Lisitskiy, and Ye. V.
 Sisakyan. Study of KRS crystal properties in the
10 μ spectral range. KE, no. 4, 1975, 765-772.

Crystal systems of the KRS-5 (TlBr-TlI) and KRS-6 (TlBr-TlCl) systems show good transparency in the 10 micron range, and so appear good candidates for CO₂ laser optics. The authors describe extensive tests on these materials, using locally grown single crystals rather than imported specimens. Tests on refraction coefficient gave values on the order of 10⁻⁴ - 10⁻⁵; transmissibility was constant over a 20-200 C temperature range. Other thermal as well as mechanical characteristics of both KRS types are tabulated.

Breakdown test were done on a number of KRS disc targets of 30-60 mm diameter and 10 mm thick, using a 70 w CO₂ laser with special controls to maintain constant emission parameters. Results showed that better than 50% of the KRS-5 specimens showed absorption coefficient α below 10⁻²/cm; for KRS-6 this figure was 80%. Some specimens reached $\alpha = 3 \times 10^{-3}$ /cm. Within measurement limits, α was not affected by crystal orientation, cut, or its type of growth atmosphere.

Both c-w and pulse tests were made of breakdown threshold; the pulsed mode used spiral electrodes to get 1--2 j pulses of 250 ns length. Radiation was focused to a 1 cm spot on the crystal surface; pulse rate was 1 Hz. Table 1 lists the thresholds for both c-w and pulse regimes for KRS-5 and -6. Typical examples of pulsed and c-w damage are shown in

Table 1. Laser Strength of KRS Crystals

Test conditions		KRS-5		KRS-6	
		Power density 10 ⁷ w/cm ²	Energy density j/cm ²	Power density	Energy density
Pulsed	on surface	7 ₊₄	10 ₊₅	3 ₊₂	6 ₊₄
	internal	16 ₊₂	24 ₊₂	10 ₊₁	20 ₊₂
c-w	on surface	-	-	10 ⁴	-

Fig. 1 and a discussion is given on the observed effects.



Fig. 1. CO₂ laser destruction of KRS crystals.

a- KRS-5, pulsed mode, x200; b- KRS-6, c- detail of crater from c-w test, x1000.

The authors conclude that KRS crystals show promise for high quality laser optics in the 10 μ range; they could be used as the exit mirror for CO₂ lasers at moderate energy levels.

3. Semiconductor Targets

Bredikhin, S. I., Yu. A. Osip'yan, and S. Z. Shmurak. Effect of light on stimulated emission from deformation in ZnS crystals. ZhETF, v. 68, no. 2, 1975, 750-755.

Photoluminescence of ZnS:Cu and ZnS:Mn single crystals, simultaneously stressed to above the elastic limit and flash-illuminated, was studied experimentally. The intent was to verify the hypothesis that illumination affects characteristics of strain-induced luminescence at the same time as it produces a photoplastic effect. Luminescence of the stressed crystals illuminated by a Xe flashlamp was recorded simultaneously with measurements of residual strain ϵ and temperature T.

The main experimental finding is that crystal illumination causes change in the N/N_c ratio, where N and N_c are the numbers of luminescence flashes per unit time in dark and during monochromatic illumination respectively. The $N/N_c = f(\lambda)$ curves exhibit minima and maxima which correspond to the maxima and minima of N_c ; hence the patterns of N/N_c changes are different in different spectral regions. There is a linear relation between N and ϵ . The $N/N_c = f(\lambda)$ dependence is correlated with the $N/N_c = f(T)$ dependence. The main experimental result shows a good qualitative agreement between spectral dependence of luminescence inhibition and the photoplastic effect data. The magnitude of the photoplastic effect and efficiency of luminescence inhibition N/N_c depend on illumination λ , its intensity, and T. The N/N_c ratio decreases or increases by illumination, depending on whether excitation λ corresponds to a spectral region of impurity (Cu, Mn) absorption or band-to-band absorption, respectively. A possible mechanism of the observed effect is outlined.

Brodin, M. S., I. L. Romanenko, and I. Yu. Shabliy. Changes in photoelectric properties of CdS single crystals after the action of laser pulses. FTP, no. 7, 1975, 1418-1419.

Laser-induced changes in photoelectric properties of solid high-resistivity CdS single crystals with low photosensitivity were experimentally investigated. Their dark resistance at 300 K was 10^{10} ohm x cm; V-A characteristics were ohmic up to field gradients of 5×10^3 v/cm.

A nonpolarized light beam from a Q-switched multimode ruby laser was focused by a lens with $f = 15$ cm on specimen crystals, normal to their hexagonal axis. Pulse duration was 20 nsec and power density P was varied from 10^7 to 10^8 w/cm². At $P = 6 \times 10^7$ w/cm², burn spots were observed on the polished specimen surfaces at the point of laser light incidence, and at $P \geq 10^8$ w/cm², crater-type defects were seen in some crystals. Changes in stationary photoelectric characteristics of the test crystals, observed after exposure to several laser pulses at $P = 6 \times 10^7$ w/cm², were as follows:

1. Photosensitivity of the crystals increased considerably while their dark resistivity did not undergo any significant change.
2. CdS crystals acquired the ability to switch to a higher conductivity in electric fields $= 5 \times 10^2$ v/cm.
3. Relaxation kinetics of photoconductivity after excitation by the usual lamp heating was significantly altered.

Some results are shown in Figs. 1 and 2. Experiments showed that in passing a laser beam of even relatively small flux density through CdS single crystals, defects are formed in them, which are capable of changing their photoelectric properties very significantly.

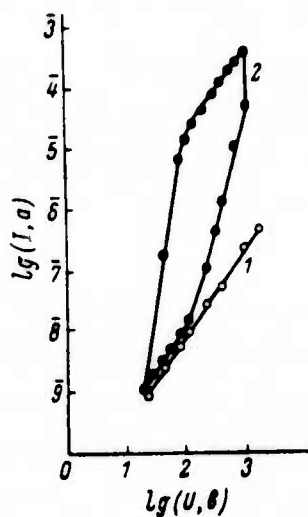


Fig. 1. V-A characteristics of CdS single crystals at 300 K before (1) and after (2) irradiation by three laser pulses. (Pulse power = 6×10^7 w/cm²).

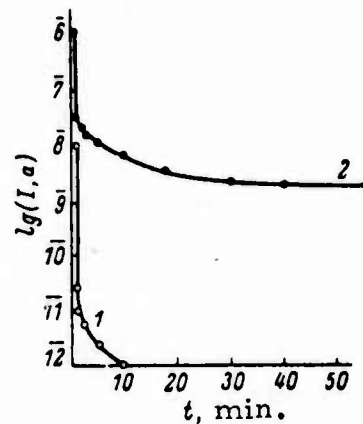


Fig. 2. Relaxation of photoconductivity in CdS at 77 K before (1) and after (2) irradiation by three laser pulses. ($P = 6 \times 10^7$ w/cm²).

Vaytkus, Yu. Yu., and K. Yu. Yarashyunas.
Self-diffraction of light by a photoinduced phase lattice in CdSe. Litovskiy fizicheskiy sbornik, v. 14, no. 6, 1974, 1001-1003.

Self-diffraction of a laser beam by a lattice made up of non-equilibrium current carriers in CdSe single crystals was experimentally investigated. The test setup is shown in Fig. 1. Radiation source was a

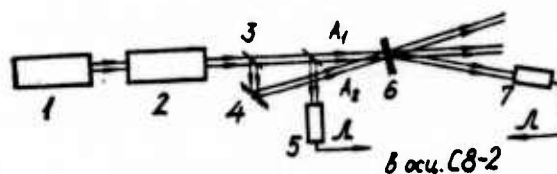


Fig. 1. Experimental setup for observing dynamic phase lattice in CdSe.

1- Neodymium laser; 2- laser amplifier; 3, 4- splitters; 5, 7- photodetectors; 6- CdSe specimen.

solid pulsed neodymium laser. Angle between beams A_1 and A_2 (Fig. 1) was varied from 2 to 4° . Incident power on specimens was 0.3 - 50 Mw/cm² with a pulse duration of 50 nsec. Intensity of the diffracted beam was measured at different excitation levels.

It was seen that at comparatively low excitation levels (up to 3-5 Mw/cm²) only scattered light falls on the photodetectors (Fig. 1). With an increase of incident pulse energy, intensity of diffraction rapidly increases as a result of optical generation, ultralinearly depending on its intensity (two-photon transitions); but further excitation of fast recombination channels lowers the performance index. Intensity of diffraction also decreases with the increase of the angle between A_1 and A_2 beams.

Variation in the ratio between incident beam intensities changes the modulation level of interference, and consequently the diffracted beam intensity. Experiments verified that the intensity of the diffracted beam strongly depends on the rate of generating non-equilibrium current carriers, and on their concentration in the lattice.

Vitkin, E. I., and Nguen Min'Khiyen.

Development of thermal breakdown with time
in semiconductors exposed to laser radiation.

DAN BSSR, no. 6, 1975, 502-505.

This study deals with laser breakdown of semiconductors, including effects of intensive light pulses, heat exchange conditions at the boundary, and specimen geometry during breakdown. The problem is theoretically studied by means of the method developed in a previous work by Vitkin (DAN BSSR, no. 12, 1965). Two cases are considered: (1) when normal incident light falls on the surface of a specimen in the form of an

infinite plane plate of thickness $2H$; and (2) when the specimen has a cylindrical form with radius R and length L , such that $L \gg R$.

Analyses are then given of conditions for breakdown in both types of geometry, as defined by several empirical factors involving beam and target parameters.

Zolotukhin, A. A., L. I. Ivanov, L. S. Milevskiy, Ye. G. Prutskov, and V. A. Yanushkevich. Effect of laser radiation on the state of a solid solution of iron and silicon. Kvantovaya elektronika, no. 2, 1975, 417-419.

Formation of defects in silicon under high density laser radiation (10^8 w/cm²) was investigated. Specimens used were: (a) n-type silicon single crystals with resistivities of 50 to 70 ohm x cm and doped with phosphorus; (b) p-type Si with specific resistance of 18 to 21 ohm x cm, doped with boron. Oxygen content in the crystals was $(1-5) \cdot 10^{17}$ cm⁻³ and dislocation density - less than 10^3 cm⁻². Specimens were irradiated in distilled water in the [111] direction by a ruby laser at room temperature. Pulse duration was ~ 50 nsec; energy was varied in intervals of 0.1 joule by means of filters. The target surface of the crystal specimens was protected from direct effects of radiation and plasma by a 25μ metallic foil, radiation being focused on the foil surface to a 2 mm spot. Electrical conductivity of the crystals was measured by a four-probe method and their Hall emf, by a compensation method in a constant 10 koe magnetic field.

Experiments were conducted with two series of specimens:

Series I - Undoped silicon crystals,

Series II - Silicon crystals doped with iron.

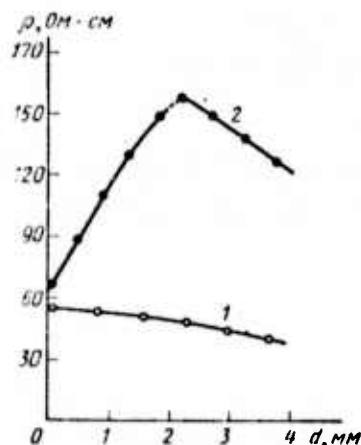


Fig. 1. Change of resistance with depth in n-Si specimens before (1) and after (2) laser irradiation with $E = 0.7$ joule.

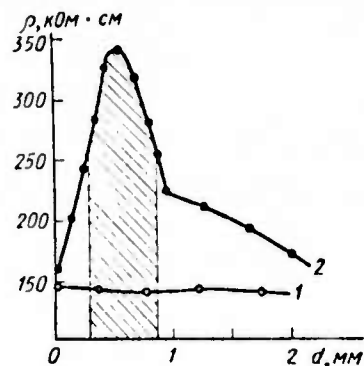


Fig. 2. Change of resistance with depth in p-Si specimens before (1) and after (2) laser irradiation, $E = 0.8$ joule.

Figs. 1 and 2 show the change of resistance with depth of n- and p-Si of series II respectively. Results indicated practically no change in resistance of the series I specimens during experiments, conductivity of these specimens was found constant up to breakdown threshold at pulse energy = 1.5 joule. In case of the series II specimens, n-Si crystals show maximum resistivity at a depth of 2 mm, then decreasing gradually. The decrease in resistivity is very pronounced in p-type specimens of the II series.

It is suggested that the increase of resistivity in n-type specimens of series II is due to the transition of iron atoms, weights of which are 2 times heavier than those of silicon, from interphase to crystalline lattice points, forming acceptor centers. Decrease of conductivity in p-Si specimens (series II) is associated with the displacement of boron atoms in the interphase state as a result of the interaction between adjacent iron and boron atoms. Different effects of radiation on electrophysical characteristics in series I and II specimens confirm that the presence of iron atoms in crystals facilitates radiation defect formation in silicon. These tests demonstrate for the first time that stress waves generated by laser radiation can lead to local changes in atomic positions of different elements in the crystal lattice of a solid.

Amigud, Z. G., I. Ye. Bolotov, F. I. Bragin,
L. V. Rabinovich, and S. B. Fischeleva.

Structural changes in zinc sulfide films during
electron and laser irradiation. OMP, no. 1,
1975, 51-54.

Changes of initial structures and damage characteristics were investigated of single-layer ZnS films, exposed to laser radiation and electron beams of varying intensity. Films were obtained by vacuum condensation of ZnS on a polished type K8 optical glass. Laser irradiation was with a solid laser (unspecified) operating at 1.06μ and a pulse duration of 40 nsec. Structures of the films were studied by transmission electron microscopy combined with microdiffraction, which yielded data on phase components as well as texture of the films. Figs. 1 and 2 show laser effects for energies below and above threshold.



Fig. 1. Microcraters formed in ZnS from pulsed energy below damage threshold.



Fig. 2. Micropores in a recrystallization zone; energy density above threshold ($\times 17,000$).

Experimental observations showed that the destruction process of ZnS films by laser radiation consists in formation of initially

micro-, and then macro-holes as beam energy is increased. Recrystallization and phase transitions occur at temperatures of 1000-1100 C, which indicates that the films have undergone thermal effects. Thermal effects could be due to plasma, the occurrence of which is always followed by the formation of macrocraters. The film substrate near crater regions were seen to be fused; consequently, thermal effects during irradiation could be also related to the heating of the films from the substrate side.

In contrast, irradiation of ZnS films by electron beams of low intensity does not cause structural changes in them. Increase of beam intensity leads first to recrystallization, followed by growth of grains and phase transitions, and finally to evaporation of the irradiated films.

Dogadov, V. V., B. A. Raykhman, and V. N. Smirnov. Change in transmissibility near the absorption edge in doped GaAs, from pulsed radiation at 10.6 μ ZhTF P, v. 1, no. 5, 1975, 251-255.

Laser-induced change in transmissibility of a p-GaAs target ($p = 10^{18}/\text{cm}^3$) was measured and analyzed. The test used a pulsed CO₂ laser, focused at $f = 300$ mm on a polished GaAs specimen 2.5 mm thick. An auxiliary optical probe using a flashlamp was focused at the center of the laser beam spot to measure the laser effect on optical transmission through the specimen, as shown in Fig. 1. The drop in transmitted probe signal as laser peak power is increased is shown in the relative curves of Fig. 2. A theoretical analysis for the recorded absorption phenomena is given. The test results can also be used to evaluate change in target surface temperature during the laser pulse. In the present case, with incident density of 20 Mw/cm², the temperature rise at pulse peak (0.05 μ s) was 50 K, and 500 K by the end of the pulse.

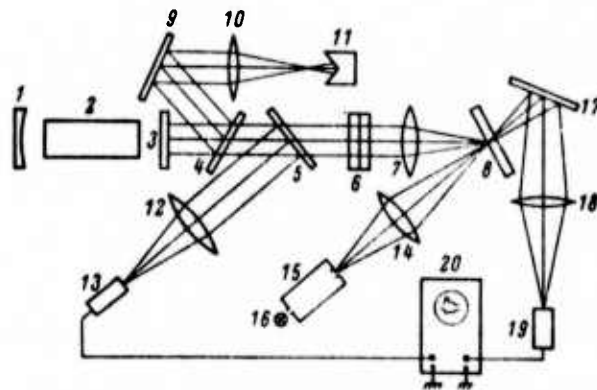


Fig. 1. Optical test setup.

1, 2, 3- CO₂ TEA laser; 4-7, 9, 10, 12, 14, 17, 18- optics; 8- GaAs specimen; 11- calorimeter; 13- photomultiplier; 15- monochromator; 16- flashlamp; 19- pyrodetector; 20- oscilloscope.

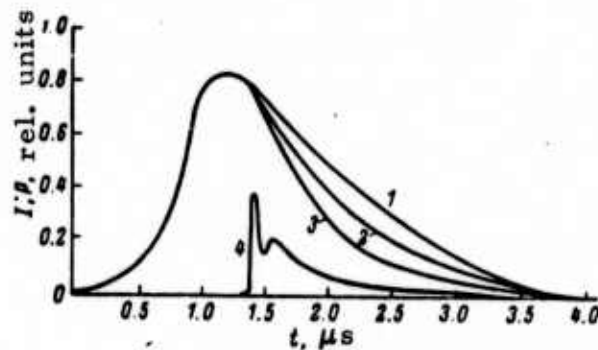


Fig. 2. Time characteristic of probe intensity vs. time for increasing laser power P.

1- $P_1 = 0$; 2- $P_2 \neq 0$; 3- $P_3 > P_2$; 4- laser pulse.

Pilipovich, V. A., G. D. Ivlev, Yu. F.
Morgun, N. V. Nechayev, V. I. Osinskiy,
and A. Ya. Peshko. Forming p-n junctions
in gallium arsenide by laser radiation. ZhPS.
v. 22, no. 3, 1975, 431-437.

A laser method for forming junctions in n-GaAs is described, using a zinc film on a polished GaAs substrate. Both a Q-switched ruby and an Nd glass laser were used in a variety of modes and pulse energies, to determine optimum conditions for junction formation. Specimen preparation and test parameters are discussed in detail.

Best results were obtained with the ruby laser, at pulse energies in the 0.3-0.4 range. At higher energies the laser damage was sufficient to degrade junction parameters. Using a train of 10 to 15 regular pulses, the authors developed junctions with inverse breakdown levels as high as 100 v. The Nd glass laser was less successful, since the gallium arsenide substrate is transparent to IR and the heat load is born mainly by the zinc film, resulting in a lower quality junction.

The effectiveness of the doping technique is a tradeoff against the tolerable laser damage to the junction area. Fig. 1 shows samples of the effects for three different lasing modes. However, with careful controls, the method is concluded to be a promising one for junction formation.



Fig. 1. Laser interaction on GaAs with Zn film.
a- free running; b- giant pulse; c- pulse train. Magnification x60.

4. Miscellaneous Studies

Kaminskiy, V. V., A. I. Shelykh, T. T.
Dedegkayev, T. B. Zhukova, S. G. Shul'man,
and I. A. Smirnov. Metal-to-semiconductor
phase transition in SmS under laser irradiation.
FTT, no. 5, 1975, 1546-1548.

Metal-to-semiconductor phase transition under laser radiation was experimentally investigated in SmS metallic layers, and the possibilities were studied of using these layers as an information recording medium. Single crystals and polycrystals of SmS films, deposited in vacuum, were considered. Possible methods of obtaining metallic modification on their surface was described in the works of Bzhalava, et al. (FTT, 16, 3753, 1974) and Volkonskaya, et al. (FTT, 17, v. 4, 1975).

Specimen surfaces were irradiated by a pulsed ruby laser in air at room temperature. Above a certain threshold energy, dark spots were formed at areas of beam incidence with the metallic surface. Experimental verification showed that these dark spots were semiconducting modifications of SmS. This phase transition of metal to semiconductor was judged to be most probably connected with the thermal action of light. Approximate calculations of the temperature to which the films were heated during laser irradiation gave T values of 600 C.

The existence of both semiconductor and metallic phases at room temperature and atmospheric pressure, together with the large differences in absolute values of light reflection coefficient of metallic and semiconductor phases, make SmS attractive as a recording medium for information storage. Experiments showed that the maximum packing density can reach 1.4×10^7 bits/cm², and maximum radiation energy required for this was ~ 0.3 joule/cm² at a pulse duration of 0.5-0.8 msec. It was also noted that the quality of recording on SmS does not deteriorate with long storage life under normal conditions.

Gusev, A. V. Origin of thermoelastic stress and temperature waves from the effect of an electromagnetic pulse of finite duration.

Problemy prochnosti, no. 2, 1975, 8-11.

During incidence of electromagnetic pulses on a solid, a portion of the radiant energy is absorbed by the surface layer. The energy thus absorbed acts as a distributed heat source over the surface and a temperature field with high gradients is generated. This leads to the development of thermal stresses, which propagate inside the substance. At sufficiently short and powerful pulses, these stresses become very significant.

The present work investigates the above problem theoretically by means of a thermoelastic model. It is assumed that the radiation pulse duration t_d is comparable with the propagation of stress waves through the absorbing surface layer. Values of maximum and minimum stresses at finite pulse durations are determined and expressions are derived for temperature waves, propagating together with stress waves. Since it is known that the characteristic time of those wave processes is by several times smaller than that of thermal conductivity, thermal conductivity is assumed absent and heat exchange with the ambient medium on the surface can also be neglected.

Apollonov, V. V., A. I. Barchukov, N. V. Karlov, A. M. Prokhorov, and E. M. Shefter.
Thermal effect of high-power laser radiation on a solid surface. KE, no. 2, 1975, 380-390.

In a study on laser thermal effects, the nonstationary temperature and thermoelastic stress fields created in an irradiated solid are determined. The object is to explore ways of increasing resistance of

laser resonator elements to thermal deformation and enhancing the capability of materials to withstand significant laser radiation intensity.

The temperature field $T(r, z, t)$ and thermoelastic stress field σ_{ij} are formulated for a semi-finite model of a strongly absorbing elastic isotropic solid in an (r, z) Cartesian coordinate system. An axisymmetric laser beam, e. g. the beam from a CO_2 single-mode laser, is assumed to be perpendicular to the target surface and beam dimension $\omega \ll L$, the dimension of the solid. The cited formulas are used to calculate radial $T(r)$ and $\sigma_{ij}(r)$ profiles and axial $T(z)$, $\sigma_{zz}(z)$ profiles for assumed Al and gold-plated quartz samples exposed to a 1 kw laser beam with $\omega = 0.2$ to 1 cm. Also, radiation threshold intensities $I_{T=T_m}$, $I_{\sigma=\sigma_f}$ and $I_{V=V_t}$ for melting, plastic flow, and tolerable deformation of the reflecting surface respectively, are calculated as functions of laser pulse length, t_0 . It is shown that $I_{T=T_m}$ is 1.5 to 2 orders of magnitude higher than $I_{\sigma=\sigma_f}$, and hence, an optical surface can crack from the effect of laser radiation at a significantly lower I than $I_{T=T_m}$. At $t_0 \geq 2 \times 10^{-3}$ sec, elastic deformation of the reflecting surface is the main I limiting process.

At $t_0 \leq 2 \times 10^{-3}$ sec, transition to a nonelastic state as the result of residual stress from irradiation is the predominant process. The I_{thr} value can be increased by selecting appropriate parameters of radiation and material, and by varying the surface reflection and coefficient of thermal conductivity of the material according to a predetermined law.

Karamzin, Yu. N., and A. P. Sukhorukov.

Mutual focusing of intense light beams in media with quadratic nonlinearity. ZhETF, v. 68, no. 3, 1975, 834-847.

Results are described of numerical experiments on investigation of resonant three-photon interaction of a confined light beam during strong

energy exchange. From experiments with Gaussian beams having no initial divergence a number of new phenomena were observed for the first time. Parametric diffusion of beams and anomalous diffraction were recorded under linear conditions of parametric amplification. During the diffraction process the wave with the higher frequency acquires a converging wave front.

The phenomenon of simultaneous focusing was discovered under conditions of strong energy exchange between beams. The field intensities in the nonlinear focus exceeded the initial intensity of the main wave by one or two orders of magnitude. During mutual focusing, which is of a quasiperiodic nature, Gaussian beams acquire a ring structure. Conditions are obtained for self-capture of beams into coupled wave guides, and structures of some stationary waves are obtained. Threshold intensity of the main wave is estimated for observing these effects in laser experiments with crystals.

Krylova, T. N., R. S. Sokolova, I. F.
Bokhonskaya, I. V. Yegorenkova, and A. Ya.
Kuznetsov. Radiation resistance of oxide
coatings, obtained from solutions. OMP, no.
12, 1974, 57-59.

Methods of improving the radiation stability of various oxide films, obtained from solutions of easily-hydrolyzable compounds, were investigated. The films considered were SiO_2 , TiO_2 , ThO_2 , HfO_2 and ZrO_2 , whose physico-chemical characteristics are tabulated. The radiation source was a ruby laser, operating in single-pulse regime at 40 ns pulse width. In a general summary of results, the threshold destruction of the target films

was found to depend significantly on their thermal stability. Purity and uniformity of film structures were also important factors affecting their destruction. The authors point out that the nature of radiation destruction of films is quite complex and requires further investigations.

Malyarovskiy, A. I., O. G. Semenov, K. F. Shipilov, and T. A. Shmaonov. Investigating scattering of a ruby laser pulse on the surface of liquefied carbon dioxide. IN: Tr. Mosk. fiz. - tekhn. in-ta, Ser. obshch. i molekulyar. fiz., no. 5, 1974, 195-200. (RZhF, 3/75, #3D1279). (Translation)

Scattering of ruby laser pulses on a liquefied CO₂ surface was investigated in a free generation regime where maximum power density = 1.8×10^5 w/cm². Measurements made included the spatial distribution of the scattered pulse intensity; the relationship of scatter intensity to incident pulse intensity; and the time dependence of the ratio between scattered and incident pulses. Possible scattering mechanisms are discussed, including thermal defocusing; surface curvature due to laser pulses; and stimulated surface scattering. It is concluded that for accurate identification of the scattering mechanism, it is necessary to study spectral components of the scattered pulse.

Pivovarov, V. M. The 3rd All-Union conference on the physics of optical radiation interaction with condensed media. OMP, no. 5, 1975, 70.

A general summary is given of the 3rd All-Union conference held in Leningrad from November 12-15, 1974 on the physics of optical radiation interaction with condensed media. The conference was organized

by the Vavilov State Optical Institute and FIAN. Some 97 reports were presented in both plenary and sectional meetings.

Reports presented in the plenary sessions were on optical stability of a medium; use of laser radiation for stimulating thermonuclear reactions; application of lasers in medicine, technology and for stimulating chemical reactions.

Problems of laser radiation interaction with glasses, laser materials and methods of improving beam stability of optical materials were discussed in the first sectional meeting. The second session dealt with two problems: 1) Study of a laser plasma, generated by laser interaction with solid targets, and 2) Study of laser radiation interaction with semiconductors.

Veyko, V. P. Laser methods for preparing scales, grids and other analogous optical components.
OMP, no. 11, 1974, 64-66.

The article describes laser techniques, presently in use or proposed, for production of scales, grids, photographic patterns, masks, and similar optical elements. Almost all information presented in the article is from Soviet open sources.

Characteristics and capabilities of the projection, radial outlining, and projection outlining techniques of optical imaging are discussed. The Soviet-made Kalan system and its EM-535 modification with Q-switched laser are cited as the most successful applications of projection techniques to production of metallized photographic patterns and bimetallic stencils. The laser systems used for obtaining optical elements by radial outlining techniques are reviewed. The most successful Soviet systems use the LGI-21

and Signal-2 molecular nitrogen lasers, the OKG-15 and LG-22 CO₂-N₂-He lasers. The purely thermal, thermochemical, and photochemical effects of laser radiation on materials are cited as the mechanisms of the imaging process. A classification of these laser techniques, which was devised by Veydenbakh (OMP, no. 9, 1972, 60) on the basis of optical elements designation, is tabulated.

Presently, processing of thin metallic films on a glass or other substrate to produce various elements is considered to be the most important application of laser techniques. Advantages of these techniques are listed.

Uglov, A. A. Characteristics of heating anisotropic materials by concentrated sources.
FiKhOM, no. 1, 1975, 152-154.

In a brief study, the effects of anisotropy in thermophysical properties of materials on the maximum value of temperature attainable on their surface, are theoretically presented, and some calculated results are plotted. Results show that for most substances, anisotropy in their thermophysical properties does not have much effect on the value of maximum temperature. However it affects very significantly the value of temperature gradient and, consequently, thermoelastic stresses.

Uglov, A. A. Proceedings of the seminar on physics and chemistry of material processing with concentrated energy fluxes. FiKhOM, no. 1, 1975, 165-166.

The 45th regular seminar on the title subject was held December 6, 1973 at the Baykov Institute of Metallurgy and was chaired by

Academician N. N. Rykalin. The seminar, attended by over 80 representatives of different organizations from several Soviet cities, dealt with the general subject of laser beam interaction with materials. The contents of five papers presented at the seminar are summarized.

Two theoretical papers were given by a team of Moscow scientists headed by S. I. Zakharov, and Yu. N. Lokhov. They analyzed the mechanism of surface breakdown of transparent dielectrics from a focused giant laser pulse, and evaluated avalanche development in solid dielectrics. Another theoretical paper, given by I. P. Dobrovolskiy and the author, analyzed heating of a semi-finite solid by a laser source. Experimental data were reported and analyzed by V. G. Andreyev et al. on formation of smooth-wall craters in transparent glasses from the effect of a 1.06μ laser beam, and by Dobrovolskiy et al. on development of the breakdown region in nitrogen above a 2 mm thick steel or molybdenum plate target, exposed to an Nd laser beam at 10^6 w/cm² power density. The effects of high pressure ambients to 100 atm on the beam-target interaction were also examined in the latter paper.

5. Laser-Plasma Interaction

Arzuov, M.I., A.I. Barchukov, F.V. Bunkin,
V.I. Konov, and A.M. Prokhorov. Self-ignition
of a continuous optical discharge in gas near
solid targets. KE, no. 5, 1975, 963 - 966.

This article discusses the initiation of a stable optical discharge in xenon by evaporation of an impure surface layer from a solid target, under the action of c-w CO_2 laser radiation. The experimental sketch is shown in Fig. 1. The CO_2 laser was used single-mode with an output power of 1 kw. Radius of the minimum focal spot $a_0 = 65\mu$, such that at full output power the average intensity of light flux on the specimen surface S was $6.5 \times 10^6 \text{ w/cm}^2$, while intensity at the beam axis S_0 was $1.5 \times 10^7 \text{ w/cm}^2$. The target surface was placed at 45° to the laser beam, so that motion of the laser flare was offset from the incident laser beam. Experiments were conducted in xenon at pressures of 10^{-3} to 1 atm.

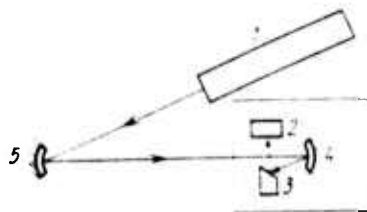


Fig. 1. Self-ignition experiment. 1 - CO_2 laser; 2 - absorber; 3 - target; 4, 5 - mirrors with curvature radius 2.5 cm and 2.5 m respectively.

At $p > 0.3$ atm., a continuous optical discharge occurred, whose plasma region extended along the curvature of the focusing lens. The plasma region thus generated remained stable even after removing the target from the laser beam, thus showing that the target served only as an initiating agent for the optical discharge in xenon. Initiation of this discharge was further found to be associated with the evaporation of an impure surface layer and not of the material itself. Targets used were duralumin and tungsten.

The following mechanism for the self-ignition of such a continuous optical discharge is suggested. The laser beam heats the dense vapors of the target surface layer up to some temperature, causing ionization of gas surrounding the target. The ionized gas bears a radiation absorption character, and as a result, gas ionization and light absorption waves, i. e., optical discharge, propagate along the laser beam according to a mechanism of "incipient combustion". These experiments show that in the "incipient combustion" regime, xenon plasma is highly absorbing and tends to shield the target from incident radiation. The distance l of the plasma boundary from the target surface (Fig. 2) and the threshold power, P_n for a stable optical discharge in xenon (Fig. 3) are calculated as a function of the incident radiation power and gas pressure, respectively. Based on the values of P_n and l , optical thickness and plasma temperatures are determined. For xenon at $p = 1$ atm and $P_0 = 1$ Kw, $P_n = 200$ watts and $l = 1.7$ cm, $\alpha \approx 1$ cm⁻¹ and $T = 1.5$ ev.

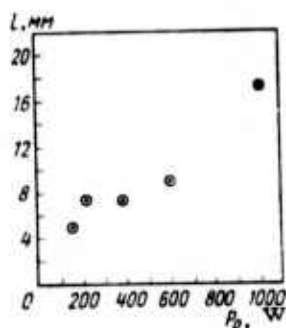


Fig. 2. Plasma boundary distance from target surface in xenon as a function of incident radiation power.

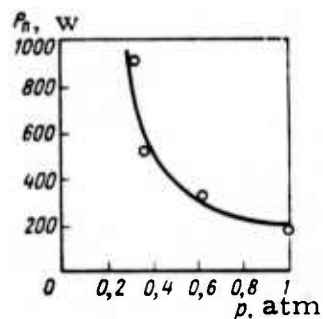


Fig. 3. Threshold power for a stable optical discharge in xenon as a function of pressure.

Bakeyev, A.A., L.A. Vasilyev, L.I. Nikolashina,
N.V. Prokopenko, A.S. Churilov, and V.I. Yakovlev.
Development dynamics and spectral component of
plasma flare radiation, occurring during the inter-
action of laser radiation with materials at $\lambda = 10.6\mu$
KE, no. 6, 1975, 1278 - 1281.

Several aspects of beam-target effects are examined. The effects of ambient air pressure surrounding the target on the interaction regime, and the development dynamics and spectral characteristics of the plasma flare generated during laser radiation interaction with materials at $\lambda = 10.6\mu$ are experimentally investigated. Targets used were graphite and duralumin; the radiation source was a pulsed CO₂ laser with radiation flux density in the 1 - 5 Mw/cm² range, at air pressures of 0.5 to 760 torr. Laser pulse duration was 3.3 μ sec and focal spot diameter was 15mm. Experimental sketch is shown in Fig. 1.

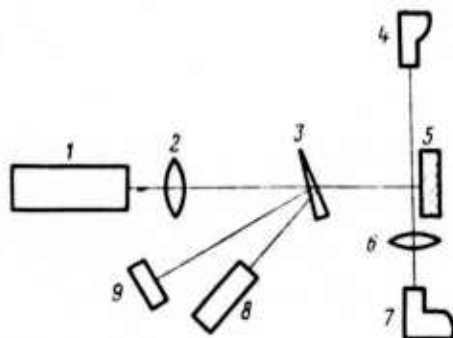


Fig. 1. Experimental sketch. 1 - CO₂ laser; 2 - lens; 3 - wedge; 4 - high-speed camera; 5 - target; 6 - lens; 7 - spectrograph; 8 - photoresistor; 9 - calorimeter.

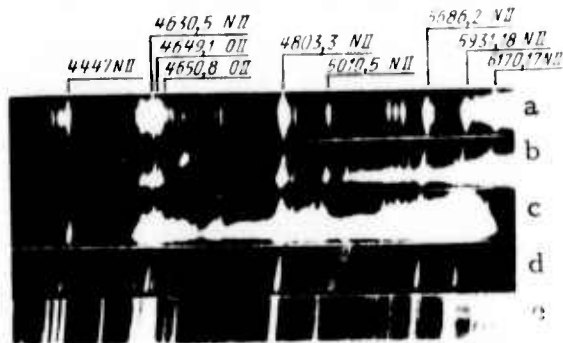


Fig. 2. Plasma flare radiation spectra at $q = 2\text{Mw}/\text{cm}^2$: a, b, c - $p = 760$ torr; d, e - 0.5 torr: a - in air; b, d - duralumin target; c, e - graphite target.

Plasma flare radiation spectra for two values of air pressure, occurring during laser radiation interaction with graphite and duralumin, and the radiation spectrum of the laser spark in air at atmospheric pressure are compared in Fig. 2. It can be seen that in all investigated ranges of radiation density and air pressure, the radiation spectra of the plasma flare for graphite and duralumin practically do not differ from one another and are close to the laser spark spectrum in air. Maximum brightness temperature T_B of the flare as a function of radiation flux density q for $L = 488\text{mm}$ and 630mm , as well as the propagation velocity v of the flare as a function of q and pressure p are plotted, for both target types. These show that the brightness temperature T_B of the plasma flare (within limits of measurement error) is independent of the target material, and is determined by the radiation flux density q . Propagation velocity of the luminous flare front at atmospheric pressure agrees well with calculations based on optical detonation theory; however, the increase of flare front velocity with the decrease of pressure takes place more slowly than theory would predict.

Burakov, V. S., and S. V. Nechayev. Active plasma diagnostics by laser radiation. ZhPS, v. 22, no. 1, 1975, 31-36.

A theoretical model of plasma diagnostics is developed and verified experimentally. Using a three-level model of the potassium atom which accounts for the most efficient resonant transitions, the authors show that absorbed laser energy saturation of a K plasma is correlated with concentration $N (=N_1 + N_k^+)$ of the plasma absorbing centers (K atoms + K^+) and initial temperature T_0 of the plasma. The energy saturation level W is attained in a plasma heated by 30 nsec laser radiation pulses at 10^7 w/cm² power density.

The formulated correlation makes it possible to calculate N and T_0 with a 10% maximum error. The absorbed energy W was measured by focusing emission from a polymethine dye laser, pumped by a single-pulse ruby laser, into a K plasma generated by electric discharge in a capillary coated with potassium. The peak power density of the focused radiation in the plasma was 30 Mw/cm². Temperature T_0 and concentration N_1 of absorbing atoms were determined spectroscopically. The experimental correlation of W with N_1 and T_0 was found to be close to theoretical. Temperature rise ΔT_e in the plasma as a function of the initial plasma parameters and W was also calculated from the energy equation.

It is concluded that N_1 and the expected ΔT_e can be evaluated from energy W absorbed by resonant transition of a readily ionized plasma component. The method can be applied to those elements with resonant transitions in the near UV, visible, and IR spectral ranges, if a tunable laser is used.

Bykovskiy, Yu. A., S. M. Sil'nov, B. Yu. Sharkov, and S. M. Shuvalov. Electrons of a laser plasma. KE, no. 5, 1975. 989-994.

Results are described of an experimental study on the electron component of a laser plasma, using a time-of-flight spectrometer method at large distances ($L = 362$ cm) from the target. The study was done on a plasma formed by the interaction of Nd laser radiation at flux density in the range of $10^9 - 5 \times 10^{11}$ w/cm² on the following targets: carbon C₁₂⁶, aluminum Al₂₇⁷⁵, manganese Mn₅₅²⁵ and tungsten W₁₈₄⁷⁵. The materials were selected to cover a broad range of atomic weights. Experimental procedures are described in detail. Angular and energetic characteristics are obtained for electron scattering, and dynamics of the formation of angular and energetic electron spectra are analyzed. Comparative analyses are conducted of the scattering characteristics of electrons and ions in the laser plasma, and mutual effects of these two components are detected during scattering of the plasma bunch in vacuum.

The authors note that the obtained results on energetic and angular spectra of the laser plasma scattering, and mutual effects of electron and ion components, are necessary for solving problems on the formation of pencil-beams of multiply charged ions for accelerators; for laser deposition of films; and are useful in explaining more thoroughly the physical picture of laser plasma scattering in vacuum.

Dabu, R., M. Isbasescu, and A. Stratan. Laser air breakdown at 1.06 μ . Rev. roum. phys., v. 19, no. 4, 1974, 391-395. (RZhF, 3/75, no. 3G266). (Translation)

Threshold values of electromagnetic energy flux density (5×10^{15} w/m²) and electric field intensity (2×10^9 v/m) were measured for air breakdown at atmospheric pressure from the effect of Q-switched Nd

glass laser pulses. Optical transmittance of the laser spark plasma is plotted versus laser radiation flux density in the lens focus.

Gol'din, V. Ya., and B. N. Chetverushkin.
Issledovaniye okhlazhdeniya i razleta
sfericheskoy misheni, razogretoy izlucheniye
lazera. (Study of the cooling and disintegration
of a spherical target heated by laser radiation.)
Moskva, 1974, 11 p. (RZhF, 3/75, #3D1265).
(Translation)

Assuming the presence of thermodynamic equilibrium, heating and scattering of a plasma was investigated by a method of numerical modelling. The plasma was obtained by irradiation in air of a CD_2 target of mass = 6.4×10^{-7} g, using laser radiation with energy = 200 joules. It was shown that ionization waves are generated in the air and propagate in front of the shock waves. According to the law of shock wave motion under high radiation conditions, it is proved that the initial plasma energy was correctly estimated.

Kaliski, S. Assessment of a laser pulse preceded
by explosion-type precompression, for the realization
of a compression of about 10^8 . Proc. Vibrat. Probl.
Polish Acad. Sci, v. 15, no. 2, 1974, 129-135.
(RZhMekh, 2/75, no. 2B244). (Translation)

A evaluation is made of possible compression of $\sim 4 \times 10^{-2}$ cm D-T solid particles for the purpose of thermonuclear fusion. Energy is assumed to be supplied to the compressed matter in the form of laser pulses.

It was found that several kilojoules of energy from a single laser pulse is required for a 10^3 compression. This amount of energy can be reduced significantly (to less than 0.4kj) by a 20 to 25-fold pre-compression during $t \approx 0.1 \mu\text{sec}$. A pulse from a relatively simpler laser can be used for this purpose. The required compression is achieved by reflection of spherical shock waves within the dense plasma cloud.

Karpov, O. V., E. F. Yurchuk, and G. D. Petrov.
Determining parameters of a plasma from the
ratio of laser radiation intensities, scattered at
different angles. TVT, no. 2, 1975, 435 - 438.

This article describes the procedure and results of experimental determination of N_e , T_e , and T_i in an argon plasmatron jet, based on scattering at different angles. The ionization level of the plasma was close to 100%; Rayleigh scattering of argon molecules was neglected. Expressions are derived for the above parameters.

The experimental system consisted of a ruby laser, modulated by a Pockels cell, and four optical systems for collecting and recording of scattered radiation at angles of 60, 90, 120, and 150°. Laser pulse power was 5Mw at a 20ns duration. Scattering volume was 1mm^3 . Spectral elements used for angles of 90 and 150° were interference filters, and for 60 and 120° -- an ISP-51 spectrograph. Backscatter of the spectrographs in the 6943 Å region was about 13 Å/mm. Parasitic illumination was two orders smaller than the scattering in plasma and calibrated signals in argon at 1 atm. Signals were detected by a photomultiplier and after amplification were recorded by oscillograph.

At high laser power densities, an increase of scattering cross-section was observed in argon, hence measurements were taken at lower power densities. Collective scattering ($T_e = 10^4\text{K}$, $N_e = 10^{16}\text{cu}^{-3}$)

was found to occur at plasmatron currents above 120 amp and $\Theta_{1,2} = 60, 120^\circ$.

I_n, a	R	n_e, cm^{-3}	$T_e, ^\circ\text{K}$	$T_e \frac{\text{Ar6416}}{\text{Ar6965}}, ^\circ\text{K}$
180	1.22	$2.45 \cdot 10^{16}$	10 500	10 800
260	1.7	$5.12 \cdot 10^{16}$	11 300	11 900

Results of two different measurements, i. e., based on ion components and on the method of relative intensity on lines ArI 6416.31 Å and 6965.43 Å are given in the table. The two results are seen to be in good agreement. It is pointed out that the method of determining parameters of a low-temperature plasma according to the ratio of laser radiation intensities, scattered at two different angles, is simple, and sufficiently reliable that it may be applied in the case of an equilibrium or nonequilibrium plasma.

Kryuchenkov, V. B. Retardation of fast ions in a plasma sphere of small diameter. KE, no. 6, 1975, 1225 - 1227.

During laser fusion in a microgram quantity of thermonuclear fuel, the problem is encountered of moderating fast ions, which are generated as a result of thermonuclear reactions in the plasma shell whose diameter d is equal to about or less than the mean free path of the fast ions in plasma ($d \lesssim \lambda$). This leads to loss of a significant portion of fast ion energy, n . The present work investigates the time dependence of the energy loss of these fast ions (α -particles) in the plasma sheath. Based on the works of Krokhin and Rozanov (Kvantovaya Elektronika, no. 4, 1972, 116), the author assumes that the determining factor for the moderation mechanism and energy loss of α -particles is the electron-ion collision. This assumption is found sufficiently true for plasma temperatures in the range of $T \leq 10\text{Kev}$. The analysis goes on to give a graphical solution for energy yield E in the plasma sphere as a function of elapsed time.

Min'ko, L. Ya. Laser plasma accelerators and plasmatrons. In: Sb. Fiz. i premeneniye plazm. uskoriteley. Minsk, Nauka i tekhn., 1974, 142 - 180. (RZhF, 5/75, #5G396).
(Translation)

This paper deals with the problem of using lasers for generating plasma fluxes. Experimental results are outlined of the action of laser radiation on absorbing materials at moderate flux densities. Particular attention is given to problems of laser radiation interaction with erosion plasma flares, and to the study of the hydrodynamic structure of laser plasma flares as a function of laser emission and interaction parameters. Different methods of plasma flux arrangements during laser interaction are analysed and some concrete laser systems for obtaining plasma fluxes are described.

Semenov, V.K., L.A. Spektorov, A.O. Sundeyeva.
Disturbance in a plasma jet during optical probing.
IN: Tr. Kirg. un-ta. Ser. fiz. nauk, no. 4, 1974,
27 - 35. (RZhF, 3/75, no. 3G291). (Translation)

A possible method is described for evaluating the disturbance introduced by an optical probe of plasma formations which are not strictly axially symmetrical. Correctness and reproducibility of plasma jet temperature fields as plotted by optical sounding are estimated. The study led to the conclusion that plasma disturbance introduced by the probe can be neglected, if thickness of the plasma ahead of the optical probe exceeds 1mm. The accuracy of the plotted temperature field should then be within 8% or better, and the systematic error of optical sounding will not exceed the magnitude of random error.

Vul'fson, Ye.K., A.V. Karyakin, and A.I. Shidlovskiy. Possibilities and limitations of the total absorption method for atomic absorption measurements in a laser flare. ZhPS, v. 22, no. 1, 1975, 14 - 19.

The minimum detectible concentration C_{\min} of elements in a target as measured by three different techniques of the total absorption (A) method with the use of a laser flare atomizer is calculated. The analysis allows for Doppler and shock broadening of a spectral line contour. First, the minimum concentration N_{\min} of atoms in the plasma is calculated as the abscissa of the break point on a theoretical rise curve of A versus N. Next, C_{\min} is determined from the assumed proportionality between C_{\min} and N_{\min} .

Using data from the literature, the authors calculated C_{\min} for Cu, Mn, and Cr in steel for UV or near-UV nonresonance spectral lines. Calculations indicate that C below 10^{-2} to $10^{-3}\%$ cannot be detected by the usual techniques of atomic absorption analysis with the use of a laser atomizer and the total absorption method. The C_{\min} threshold could be lowered at least several-fold by using a resonance line or, in certain cases, a high-dispersion spectrometer.

Zhdanov, S.K., and B.A. Trubnikov. Optimum compression of plasma in Z- and θ -pinch. ZhETF P, v. 21, no. 6, 1975, 371 - 374.

Adiabatic compression of an infinite cylindrical plasma column of finite mass is theoretically discussed. For obtaining super-high density plasma during laser heating of a target, or in a Z- or a θ -pinch, special timed shaping of the compression pulse is necessary. The optimum regime is attained under conditions in which the shock wave has not yet developed in the medium and the velocity of thermal wave propagation is small, i. e., preheating, which inhibits compression, is absent. The present work shows the possibility for adiabatic compression

of such a uniform plasma, which is not followed by development of shock waves. Calculations show that at an initial density of deuterium plasma $n_0 = 10^{15} \text{ cm}^{-3}$ and $P/n_0 = 27 \text{ ev}$ (P is initial plasma pressure), an initial internal magnetic field of the plasma $B_i = 10^2 \text{ gauss}$ is sufficient, such that the compression wave traverses throughout the nonturbulent medium ten times faster than thermal waves. Optimum laws are determined for the growth of external magnetic field (θ -pinch) and linear current (Z-pinch).

Zakharenkov, Ya. A., N. N. Zorev, O. N.
Krokhin, Ya. A. Mikhaylov, A. A. Rupasov,
G. V. Sklizkov, and A. S. Shikanov. Spatial
variation in corona density of a laser plasma at
fluxes of 10^{14} to 10^{15} w/cm^2 . ZhETF P, v. 21,
no. 9, 1975, 557-561.

Difficulties in measuring the extremely high electron densities in a developing laser plasma has led the authors to devise a combined observational method, which is described. The method was used to map the N_e profile of a laser plasma generated by 2 ns, 200 j pulses on an aluminum target, at a density of $3 \times 10^{14} \text{ w/cm}^2$. The second half of the pulse, in which a nonmonotonic N_e decay occurs in the corona, is observed in particular. Tests were run by a combination of spectroscopy and interferometry, as indicated in Fig. 1. In the range of $10^{19} - 10^{21} / \text{cm}^3$ continuous x-ray spectroscopy was used; in the $10^{18} - 10^{19} / \text{cm}^3$ range, high-speed interferometry was used with a special computer processing of the interferograms. In the critical region at $N_e = 10^{21} / \text{cm}^2$, second harmonic spectroscopy was used. Fig. 2 illustrates the growth of the luminous second harmonic area in the laser axis direction.

The separate steps of the technique are discussed in some detail, and possible reasons for the observed N_e profile are examined. The authors suggest that a sharp rise in optical pressure near the critical N_e , possibly to the order of $3 \times 10^5 \text{ atm}$, could cause a "shock" effect responsible for the ensuing N_e profile.

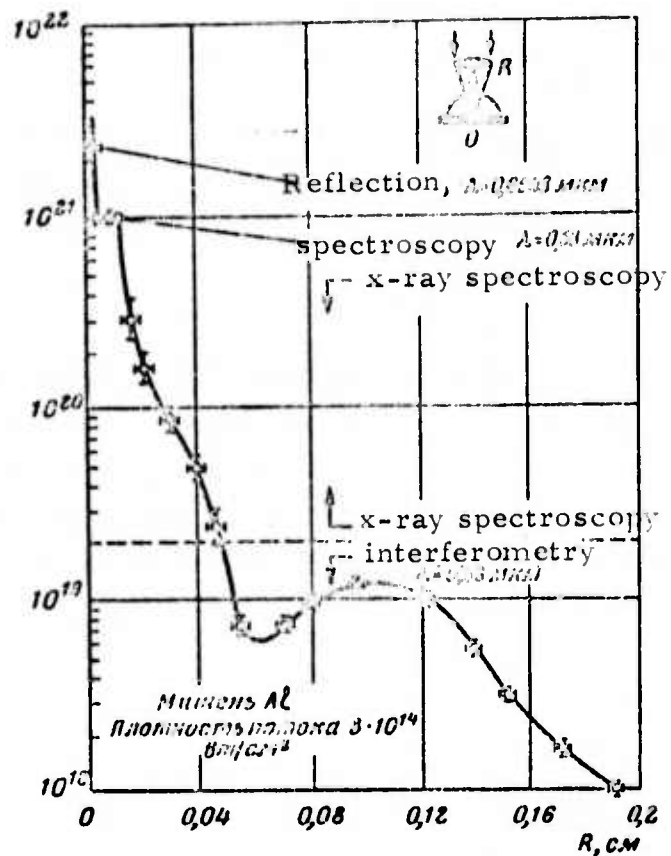


Fig. 1. Electron density profile in laser plasma, during last half of a 2 ns laser pulse.

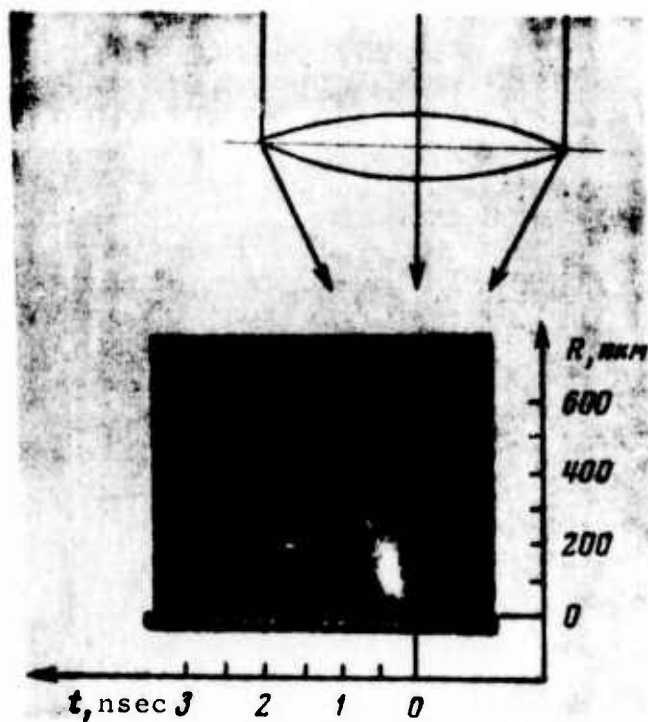


Fig. 2. Slit imaging of 2nd harmonic luminous area in laser plasma.

Gol'din, V. Ya., and B. N. Chetverushkin.
Study of cooling and dispersion of a laser-
heated spherical target. ZhETF, v. 68, no.
 5, 1975, 1708-1771.

Heating, plasma expansion and cooling are analyzed for the case of a $C_n D_{2n}$ polyethylene target exposed to a laser in air at 15 torr. Target mass was 6×10^{-7} g; laser energy was 200 j, which was assumed to impact uniformly over the spherical target. Graphical solutions are presented for various plasma parameters as functions of plasma radius and time (Figs. 1-4). The tests show that an ionization wave is formed in air

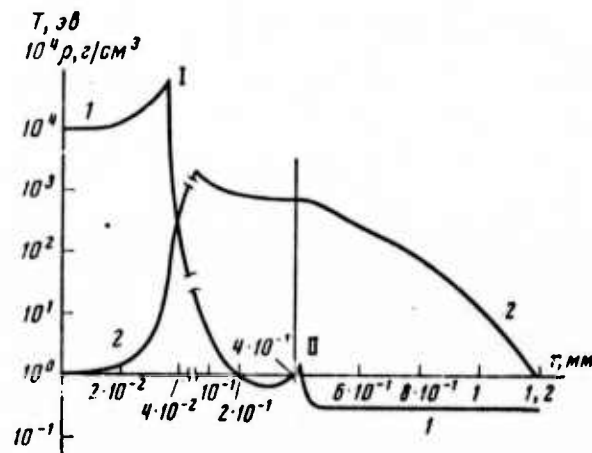


Fig. 1. Density (1) and temperature (2) vs. radius at $t = 1$ ns. Numerals I and II indicate shock wave position.

which precedes the shock wave. It is also shown that evaluating the energy of the explosion by its shock wave progression in air is applicable to the present case of powerful incident radiations.

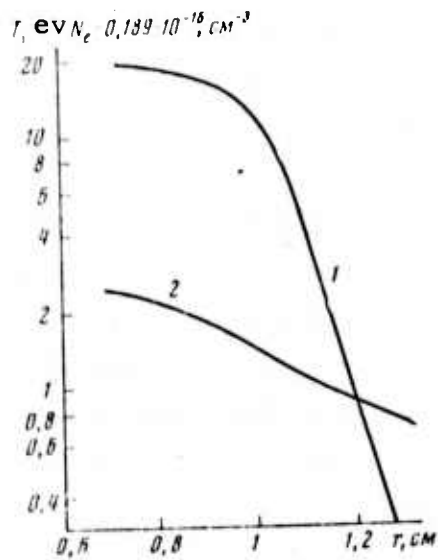


Fig. 2. N_e (1) and temperature (2) in the ionization wave region, $t = 20$ nsec.

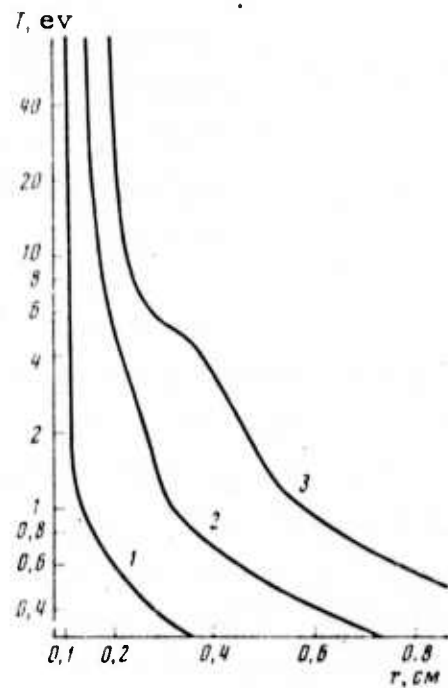


Fig. 3. Temperature variation with absorption wave motion, at times $t = (1) 1$ ns; (2) 1.4 ns; (3) 2 ns.

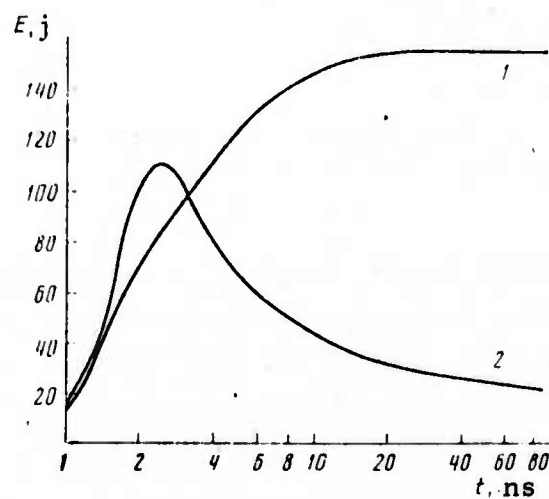


Fig. 4. Internal energy (1) and kinetic energy (2) vs. time.

Gamaliy, Ye. G., A. I. Isakov, Yu. A.
Myerkul'yev, A. I. Nikitenko, Ye. R.
Rychkova, and G. V. Sklizkov. Targets
for spherical heating and compression tests
with a laser. KE, no. 5, 1975, 1043-1047.

The authors review some recent methods for preparing spherical targets for laser fusion tests, and describe some techniques of their own. One of these has been to freeze liquid hydrogen or deuterium droplets on a suspension filament by an evacuation method. This has yielded spherical droplets of 300 to 600 μ . Metal suspension filaments proved too heat-conductive; by using rubber cement threads of 3--16 μ , the authors found that the target remained solid for several minutes at 14-20 K. Fig. 1 shows a hydrogen droplet on a 12 μ thread.



Fig. 1. Microphoto of solid hydrogen droplets on a 12 μ rubber cement filament.

To obtain hollow spheres, a commercial polystyrene foam plastic was used, from which the small percentage of free spheres was heating in boiling water, yielding shells in a range of 60 to 190 μ . The majority of these had spherical error not over 0.3% and some 30% had wall deviation below observable threshold, i.e. 0.3 μ . Both diameter and shell thickness were however found to be strongly dependent on foam bath temperature. Fig. 2 shows views of polystyrene shell.

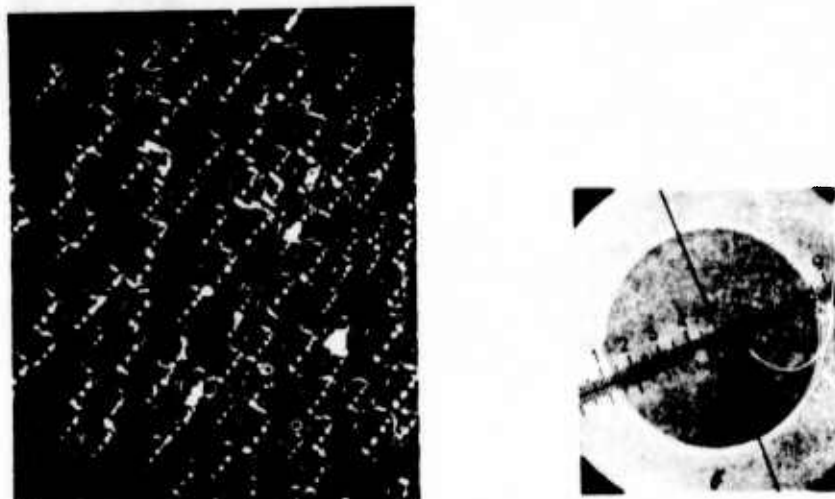


Fig. 2. Group of polystyrene shells (a);
Detail of shell (b), 1 div = 3.3μ .

While this target type has appreciably lower hydrogen content than water, polyethylene, polymethane etc., it is much simpler to produce. The two cited types with "spiderweb" suspension are therefore recommended for their technical simplicity.

Berezhnaya, V. P., G. D. Petrov, and A. I. Petryakov. Submillimeter polarimetry of a plasma in a transverse magnetic field. TVT, no. 3, 1975, 684-686.

The method of plasma diagnostics by measuring polarization changes of a beam propagating through an axial magnetic field is gaining wide acceptance. The authors show that a similar diagnostics technique can also be used for the more difficult case of a transverse field.

The theoretical basis for the transverse case is developed and verified by experiment. Tests were then run to determine electron density in a hydrogen flame, using the system of Fig. 1. For electron densities in the 10^{12} to $10^{17}/\text{cm}^3$ range and fields of 1 to 3 tesla, it was found best to use a submillimeter laser with linear polarization.

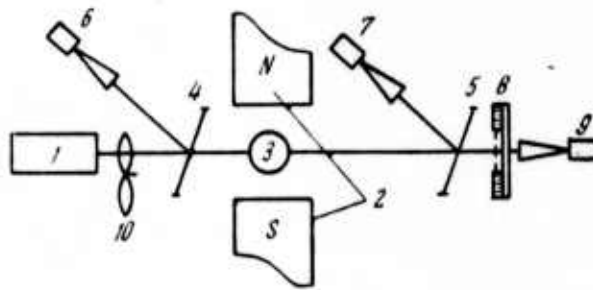


Fig. 1. Polarization method of diagnostics.

1- HCN laser, $\lambda = 337\mu$; 2- electromagnet;
 3- test plasma; 4, 5- splitters; 6, 7, 9 - detectors;
 8- parallel-wire analyzer grid.

The ratio of polarized energy passed by the plasma to total polarized energy is used to determine phase difference induced by the transverse field; from this phase difference the electron N_e is obtained. In the tests described a mean value of $4.7 \times 10^{15}/\text{cm}^3$ was found for N_e . A check against a Mach-Zender interferometer also using a submillimeter laser showed agreement within 18%. This is concluded to verify the validity of the proposed polarization method.

6. SOURCE ABBREVIATIONS

AiT	-	Avtomatika i telemekhanika
APP	-	Acta physica polonica
DAN ArmSSR	-	Akademiya nauk Armyanskoy SSR. Doklady
DAN AzSSR	-	Akademiya nauk Azerbaydzhanskoy SSR. Doklady
DAN BSSR	-	Akademiya nauk Belorusskoy SSR. Doklady
DAN SSSR	-	Akademiya nauk SSSR. Doklady
DAN TadSSR	-	Akademiya nauk Tadzhikskoy SSR. Doklady
DAN UkrSSR	-	Akademiya nauk Ukrainskoy SSR. Dopovidi
DAN UzbSSR	-	Akademiya nauk Uzbekskoy SSR. Doklady
DBAN	-	Bulgarska akademiya na naukite. Doklady
EOM	-	Elektronnaya obrabotka materialov
FAiO	-	Akademiya nauk SSSR. Izvestiya. Fizika atmosfery i okeana
FGiV	-	Fizika goreniya i vzryva
FiKhOM	-	Fizika i khimiya obrabotka materialov
F-KhMM	-	Fiziko-khimicheskaya mekhanika materialov
FMiM	-	Fizika metallov i metallovedeniye
FTP	-	Fizika i tekhnika poluprovodnikov
FTT	-	Fizika tverdogo tela
FZh	-	Fiziologicheskiy zhurnal
GiA	-	Geomagnetizm i aeronomiya
GiK	-	Geodeziya i kartografiya
IAN Arm	-	Akademiya nauk Armyanskoy SSR. Izvestiya. Fizika
IAN Az	-	Akademiya nauk Azerbaydzhanskoy SSR. Izvestiya. Seriya fiziko-tekhnicheskikh i matematicheskikh nauk

IAN B	-	Akademiya nauk Belorusskoy SSR. Izvestiya. Seriya fiziko-matematicheskikh nauk
IAN Biol	-	Akademiya nauk SSSR. Izvestiya. Seriya biologicheskaya
IAN Energ	-	Akademiya nauk SSSR. Izvestiya. Energetika i transport
IAN Est	-	Akademiya nauk Estonskoy SSR. Izvestiya. Fizika matematika
IAN Fiz	-	Akademiya nauk SSSR. Izvestiya. Seriya fizicheskaya
IAN Fizika zemli	-	Akademiya nauk SSSR. Izvestiya. Fizika zemli
IAN Kh	-	Akademiya nauk SSSR. Izvestiya. Seriya khimicheskaya
IAN Lat	-	Akademiya nauk Latviyskoy SSR. Izvestiya
IAN Met	-	Akademiya nauk SSSR. Izvestiya. Metally
IAN Mold	-	Akademiya nauk Moldavskoy SSR. Izvestiya. Seriya fiziko-tehnicheskikh i matematicheskikh nauk
IAN SO SSSR	-	Akademiya nauk SSSR. Sibirskoye otdeleniye. Izvestiya
IAN Tadzh	-	Akademiya nauk Tadzhiksoy SSR. Izvestiya. Otdeleniye fiziko-matematicheskikh i geologo-khimicheskikh nauk
IAN TK	-	Akademiya nauk SSSR. Izvestiya. Tekhnicheskaya kibernetika
IAN Turk	-	Akademiya nauk Turkmenskoy SSR. Izvestiya. Seriya fiziko-tehnicheskikh, khimicheskikh, i geologicheskikh nauk
IAN Uzb	-	Akademiya nauk Uzbekskoy SSR. Izvestiya. Seriya fiziko-matematicheskikh nauk
IBAN	-	Bulgarska akademiya na naukite. Fizicheski institut. Izvestiya na fizicheskaya institut s ANEB
I-FZh	-	Inzhenerno-fizicheskiy zhurnal

IIR	-	Izobretatel' i ratsionalizator
ILEI	-	Leningradskiy elektrotekhnicheskii institut. Izvestiya
IT	-	Izmeritel'naya tekhnika
IVUZ Avia	-	Izvestiya vysshikh uchebnykh zavedeniy. Aviatsionnaya tekhnika
IVUZ Cher	-	Izvestiya vysshikh uchebnykh zavedeniy. Chernaya metallurgiya
IVUZ Energ	-	Izvestiya vysshikh uchebnykh zavedeniy. Energetika
IVUZ Fiz	-	Izvestiya vysshikh uchebnykh zavedeniy. Fizika
IVUZ Geod	-	Izvestiya vysshikh uchebnykh zavedeniy. Geodeziya i aerofotos'yemka
IVUZ Geol	-	Izvestiya vysshikh uchebnykh zavedeniy. Geologiya i razvedka
IVUZ Gorn	-	Izvestiya vysshikh uchebnykh zavedeniy. Gornyy zhurnal
IVUZ Mash	-	Izvestiya vysshikh uchebnykh zavedeniy. Mashinostroyeniye
IVUZ Priboro	-	Izvestiya vysshikh uchebnykh zavedeniy. Priborostroyeniye
IVUZ Radioelektr	-	Izvestiya vysshikh uchebnykh zavedeniy. Radioelektronika
IVUZ Radiofiz	-	Izvestiya vysshikh uchebnykh zavedeniy. Radiofizika
IVUZ Stroi	-	Izvestiya vysshikh uchebnykh zavedeniy. Stroitel'stvo i arkhitektura
KhVE	-	Khimiya vysokikh energiy
KiK	-	Kinetika i kataliz
KL	-	Knizhnaya letopis'
Kristall	-	Kristallografiya
KSpF	-	Kratkiye soobshcheniya po fizike

LZhS	-	Letopis' zhurnal'nykh statey
MiTOM	-	Metallovedeniye i termicheskaya obrabotka materialov
MP	-	Mekhanika polimerov
MTT	-	Akademiya nauk SSSR. Izvestiya. Mekhanika tverdogo tela
MZhiG	-	Akademiya nauk SSSR. Izvestiya. Mekhanika zhidkosti i gaza
NK	-	Novyye knigi
NM	-	Akademiya nauk SSSR. Izvestiya. Neorganicheskiye materialy
NTO SSSR	-	Nauchno-tekhnicheskiye obshchestva SSSR
OiS	-	Optika i spektroskopiya
OMP	-	Optiko-mekhanicheskaya promyshlennost'
Otkr izobr	-	Otkrytiya, izobreneniya, promyshlennyye obraztsy, tovarnyye znaki
PF	-	Postepy fizyki
Phys abs	-	Physics abstracts
PM	-	Prikladnaya mekhanika
PMM	-	Prikladnaya matematika i mekhanika
PSS	-	Physica status solidi
PSU	-	Pribory i sistemy upravleniya
PTE	-	Pribory i tekhnika eksperimenta
Radiotekh	-	Radiotekhnika
RiE	-	Radiotekhnika i elektronika
RZhAvtom	-	Referativnyy zhurnal. Avtomatika, telemekhanika i vychislitel'naya tekhnika
RZhelekt	-	Referativnyy zhurnal. Elektronika i yeye primeneniye

RZhF	-	Referativnyy zhurnal. Fizika
RZhFoto	-	Referativnyy zhurnal. Fotokinotekhnika
RZhGeod	-	Referativnyy zhurnal. Geodeziya i aeros"- yemka
RZhGeofiz	-	Referativnyy zhurnal. Geofizika
RZhInf	-	Referativnyy zhurnal. Informatics
RZhKh	-	Referativnyy zhurnal. Khimiya
RZhMekh	-	Referativnyy zhurnal. Mekhanika
RZhMetrolog	-	Referativnyy zhurnal. Metrologiya i izmer- itel'naya tekhnika
RZhRadiot	-	Referativnyy zhurnal. Radiotekhnika
SovSciRev	-	Soviet science review
TiEKh	-	Teoreticheskaya i eksperimental'naya khimiya
TKiT	-	Tekhnika kino i televideniya
TMF	-	Teoreticheskaya i matematicheskaya fizika
TYT	-	Teplofizika vysokikh temperatur
UFN	-	Uspekhi fizicheskikh nauk
UFZh	-	Ukrainskiy fizicheskiy zhurnal
UMS	-	Ustalost' metallov i splavov
UNF	-	Uspekhi nauchnoy fotografii
VAN	-	Akademiya nauk SSSR. Vestnik
VAN BSSR	-	Akademiya nauk Belorusskoy SSR. Vestnik
VAN KazSSR	-	Akademiya nauk Kazakhskoy SSR. Vestnik
VBU	-	Belorusskiy universitet. Vestnik
VNDKh SSSR	-	VNDKh SSSR. Informatsionnyy byulleten'
VLU	-	Leningradskiy universitet. Vestnik. Fizika, khimiya
VMU	-	Moskovskiy universitet. Vestnik. Scriya fizika, astronomiya

ZhETF	-	Zhurnal eksperimental'noy i teoreticheskoy fiziki
ZhETF P	-	Pis'ma v Zhurnal eksperimental'noy i teoreticheskoy fiziki
ZhFKh	-	Zhurnal fizicheskoy khimii
ZhNiPFiK	-	Zhurnal nauchnoy i prikladnoy fotografii i kinematografii
ZhNKh	-	Zhurnal neorganicheskoy khimii
ZhPK	-	Zhurnal prikladnoy khimii
ZhPMTF	-	Zhurnal prikladnoy mekhaniki i tekhnicheskoy fiziki
ZhPS	-	Zhurnal prikladnoy spektroskopii
ZhTF	-	Zhurnal tekhnicheskoy fiziki
ZhVMMF	-	Zhurnal vychislitel'noy matematiki i matematicheskoy fiziki
ZL	-	Zavodskaya laboratoriya
ZhTF P	-	Pis'ma v Zhurnal tekhnicheskoy fiziki.

7. Author Index

A

Ageyev, V. A. 1
Aleksandrov, V. I. 23
Aleshin, I. V. 25, 29
Amigud, Z. G. 39
Andreyev, V. G. 26
Apollonov, V. V. 44
Arzov, M. I. 51
Ashmarin, I. I. 20

B

Bakeyev, A. A. 53
Berezhnaya, V. P. 67
Bonch-Bruyevich, A. M. 4, 27
Branov, M. S. 3
Bredikhin, S. I. 33
Brodin, M. S. 34
Burakov, V. S. 55
Buravlev, Yu. M. 5, 6
Buzhinskiy, I. M. 22
Bykovskiy, Yu. A. 56

D

Dabu, R. 56
Darvoyd, T. I. 31
Dogadov, V. V. 40

G

Gan'aliy, Ye. G. 66
Gol'din, V. Ya. 57, 64
Golubev, G. P. 15, 16
Gusev, A. V. 44

K

Kaliski, S. 57
Kats, A. V. 27
Kaminskiy, V. V. 43
Karamzin, Yu. N. 45
Karpov, O. V. 58
Krylov, K. I. 16
Krylova, T. N. 46
Kryuchenkov, V. B. 59

L

Larina, R. R. 14, 19
Lobacheva, G. Ya. 13

Lokhov, Yu. N. 26
Luk'yanov, A. T. 12

M

Malyarovskiy, A. I. 47
Min'ko, L. Ya. 60

N

Nepokoychitskiy, A. G. 9

P

Pilipovich, V. A. 42
Pivovarov, V. M. 47

S

Samsonov, G. V. 10, 11
Semenov, V. K. 60
Smirnov, V. N. 21

T

Tribel'skiy, M. I. 18

U

Uglov, A. A. 49

V

Vaytkus, Yu. Yu. 35
Veyko, V. P. 48
Vigasin, A. A. 24
Vinogradov, A. V. 18
Vitkin, E. I. 36
Vul'fson, Ye. K. 61

Z

Zakharenkov, Ya. A. 62
Zhdanov, S. K. 61
Zhukov, A. A. 8
Zolotukhin, A. A. 37